PANDA Report PV/01-07

Track following in dense media and inhomogeneous magnetic fields

A. Fontana, P. Genova, L. Lavezzi and A. Rotondi

Department of Theoretical and Nuclear Physics and INFN Sezione di Pavia
Via Bassi 6, 27100 Pavia, Italy

Abstract

We collect and explain here the basic formulae of the track following and their implementation in GEANE. Some modifications for the existing code are suggested and the results on PANDA apparatus are shown.

Contents

1 Introduction

With the words "track following", one usually intends two main tasks:

a. to transport the track parameters (particle momentum, position and direction) from one point to another in the apparatus, forward and backward. The forward part can be obtained by simply using the MC codes with the fluctuations switched off. For the backward tracking (with increasing momentum) only minor modifications of the MC codes are usually required;

b. to propagate the errors on the track parameters together with the mean values. This is usually obtained by calculating, step by step, the 5×5 error or covariance matrix of the track (see below). This mathematical part is analytically rather complicated: some general idea is given in the current literature [1] but the detailed formulae are still confined in the internal reports of the experiments, where many misprints and unclear explanations are present. Some correct approaches can be found in [2, 3].

The Monte Carlo and track fitting tasks have been treated jointly by the CERN community in the nineties. The famous GEANT3 program was used for the point a., that is for the determination of the track mean values. For the point b., the routines for the calculation and the transport of the error matrix, written by the CERN EMC collaboration [2], were interfaced with the structure, giving rise to a FORTRAN package called GEANE [4]:

GEANE = GEANT3 tracking + EMC error propagation routines.

The great advantage of this structure is that the track following is automatically obtained *with the same geometry banks of the Monte Carlo*, without the necessity to write *ad hoc* codes.

After the transition to GEANT4, the GEANE structure has been lost. Thank to the virtual Monte Carlo structure of the PANDARoot framework, the old GEANT3-GEANE chain has been recovered. It is possible that in the future a similar tool will be available also in the GEANT4 framework, as the code GEANT4E developed by the CMS Collaboration.

With this report we intend to make available, to the PANDA community, all the physical and mathematical results on which the GEANE structure is founded. Moreover, we describe in detail some important modifications that we have made to GEANE for PANDA regarding multiple scattering and energy loss. The use of the package is also explained in detail and many examples are given.

We try to demonstrate and to justify all the statements and the formulae, to create a tool for the future work. Indeed, the detailed ideas, techniques and formulae of the track following collected here, that are the basis of any track following code, are independent of any language or framework.

2 The track

The physical path of a particle of assigned mass m and momentum p is a six-fold entity of parameters x, y, z, p_x, p_y, p_z.

The track is defined as a set of points in the detectors, corresponding to the physical path of a particle.

The track points are obtained as the intersections of the particle path with what we will call detector planes, that can be real detector planes or ideal planes, in this case usually chosen perpendicularly to the particle direction.

If we translate the Master Reference System (MARS) and make the $x-y$ plane to coincide with the detector plane, the z-coordinate is blocked. This demonstrates that the track is an entity defined by five parameters (see Fig. 1). We denote with $a, b = 1, 2, \ldots, 5$ the track parameters and with $i = 1, 2, \ldots, N$ the detector plane index. Then, we write as $\boldsymbol{f} = f_i^a$ the true mean values of the track parameters at the intercept of the N detector planes and their measured values as $\boldsymbol{x} = x_i^a$.

In this report we use the notation of standard statistical textbooks: a random variable $\boldsymbol{X}$ (before the measurement) is indicated with capital letters; after the measurement, the value x assumed by the variable is indicated with lower cases (see also tab. 3). The random contents of $\boldsymbol{X}$ include measurement errors (if any) and the fluctuations coming from physical processes as energy loss and multiple scattering.

The 5×5 inverse of the covariance matrix C_i^{ab} of these measurements will be indicated with $\boldsymbol{V} = V_i^{ab}$ (weight matrix).

Usually there are different choices of the five track parameters. The most common ones, that are also codified in the GEANE package, are the following ones (see also Fig. 2) [4, 5]:

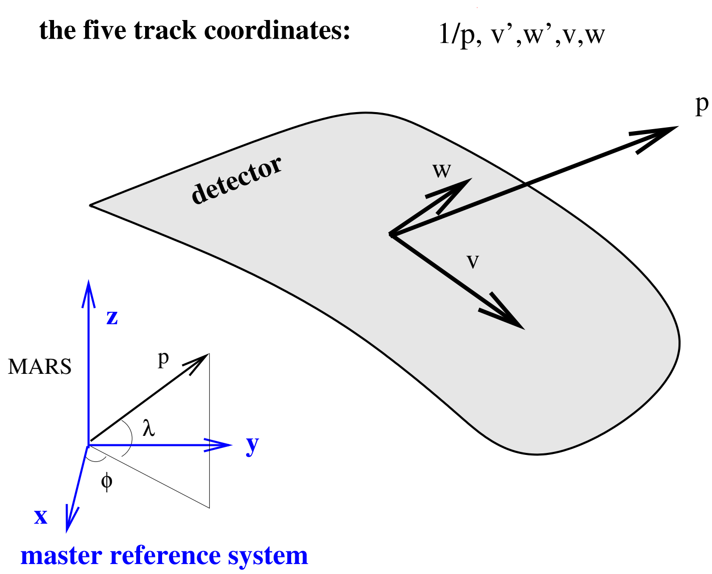

Figure 1: The five track parameters

- The transverse SC system:

$$1/p \ , \ \ \lambda \ , \ \ \phi \ , \ \ y_\perp \ , \ \ z_\perp \ , \tag{1}$$

where λ and ϕ are the dip and azimuthal angle in MARS and $y_\perp$ and $z_\perp$ are the coordinate of the trajectory in a frame with $x_\perp$ along the particle direction and $y_\perp$ parallel to the xy plane. The momentum components in MARS are given by:

$$\begin{aligned} p_x &= p \cos\lambda \cos \phi \ , \\ p_y &= p \cos\lambda \sin \phi \ , \\ p_z &= p \sin\lambda \ ; \end{aligned} \tag{2}$$

The SC $\boldsymbol{x}$ unit vector is defined along the $\boldsymbol{p}$ direction:

$$\boldsymbol{x}_\perp = (\cos\lambda\cos\phi, \, \cos\lambda\sin\phi \ , \, \sin\lambda) \ . \tag{3}$$

Since $\boldsymbol{y}_\perp$ lies in the MARS $x - y$ plane and is perpendicular to $\boldsymbol{p}$, the usual choice is

$$\boldsymbol{y}_\perp = \frac{\boldsymbol{z} \times \boldsymbol{x}_\perp}{|\boldsymbol{z} \times \boldsymbol{x}_\perp|}$$

which gives

$$\boldsymbol{y}_\perp = (-\sin\phi,\, \cos\phi,\, 0) \tag{4}$$

where $\boldsymbol{y}_\perp$ and $\boldsymbol{y}$ are oriented in the same sense; with the cross product $\boldsymbol{x}_\perp \times \boldsymbol{y}_\perp = \boldsymbol{z}_\perp$ we easily obtain

$$\boldsymbol{z}_\perp = (-\sin\lambda\cos\phi,\; -\sin\lambda\;\sin\phi,\, \cos\lambda)\;; \tag{5}$$

- the detector SD system:

$$1/p\;,\; v'\;,\; w'\;,\; v\;,\; w\;, \tag{6}$$

where (u, v, w) is an orthonormal reference system with the vw plane coincident with the detector one. The derivatives indicate the momentum direction variation in the new system. Taking into account that the directions $\boldsymbol{v}$ and $\boldsymbol{w}$ are assigned in input when the SD plane is defined, so that

$$\boldsymbol{u} = \boldsymbol{v} \times \boldsymbol{w}$$

and recalling eq. (3), we can write:

$$v' = \frac{\boldsymbol{x}_\perp \cdot \boldsymbol{v}}{\boldsymbol{x}_\perp \cdot \boldsymbol{u}} \qquad w' = \frac{\boldsymbol{x}_\perp \cdot \boldsymbol{w}}{\boldsymbol{x}_\perp \cdot \boldsymbol{u}}\;. \tag{7}$$

- the "spline" SP system:

$$1/p\;,\; y'\;,\; z'\;,\; y\;,\; z\;. \tag{8}$$

This representation is used when the detector arrays are placed along the x-axis [4].

The SD representation permits to follow the trajectory on any detector plane, real or ideal. The GEANE package allows to pass from one reference to another one through the routines TRSCSP (i.e. from SC to SP), TRSCSD, TRSDSP, TRSDSC, TRSPSC, TRSPSD [4]. These routines are in principle not necessary for the normal user, but can be called for advanced applications (see sect. 8).

In GEANE the basic transformation is from MARS to the SC system. From eqs. (3-5) the corresponding transformation matrix is

$$\begin{pmatrix} x_\perp \\ y_\perp \\ z_\perp \end{pmatrix} = \begin{pmatrix} \cos\lambda\cos\phi & \cos\lambda\sin\phi & \sin\lambda \\ -\sin\phi & \cos\phi & 0 \\ -\sin\lambda\cos\phi & -\sin\lambda\sin\phi & \cos\lambda \end{pmatrix} \begin{pmatrix} x \\ y \\ z \end{pmatrix} \tag{9}$$

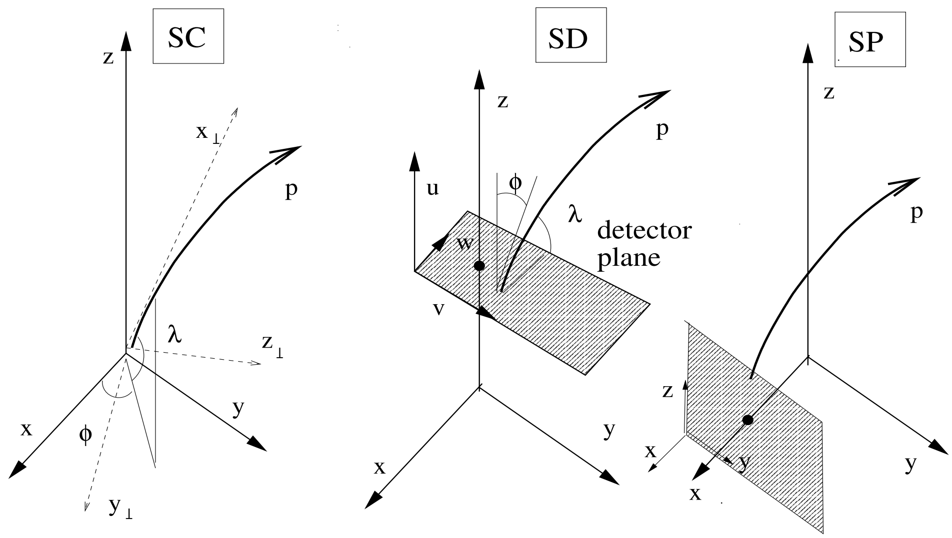

Figure 2: Systems of reference for the track following

3 Track following

The track parameters can be considered as a function of the track length l, so that we can write $f^a(l)$ or $x^a(l)$. The track follower (tracker) predicts the trajectory of a charged particle in term of mean values and errors.

During tracking, three processes are taken into account:

- energy loss, which affects both averages (the Bethe Bloch formula) and errors (called Landau fluctuations);
- Coulomb multiple scattering, that influences the error calculation only (Molière theory or gaussian approximation);
- the magnetic field, that influences the average trajectory only.

The check of the tracker should be done by simulating an ensemble of particles and verifying that the mean values and the σ's of the histograms are correctly predicted by the tracker (see Fig. 3). When one has determined the measured track value x^a or an estimate of the true track values f^a at a track length l_0, the track following code determines the value at a new value l, in the forward or backward direction. We will denote this extrapolation, which gives the

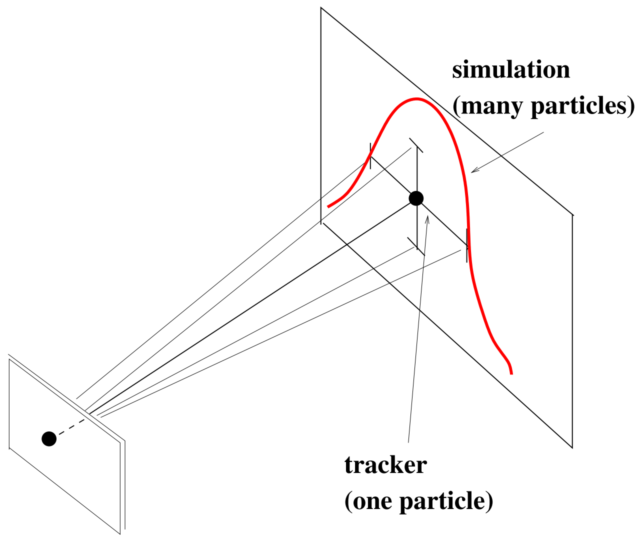

Figure 3: Comparison between the track follower and a MC simulation

parameter mean values, as an operator $\boldsymbol{G}(\cdot)$ (remembering GEANE):

$$e^a(l) = \boldsymbol{G}(l_0) \ , \qquad (a = 1, 2, \ldots, 5) \ , \tag{10}$$

where the starting point at l_0 can be chosen as $\boldsymbol{G}(\boldsymbol{f}(l_0))$ or $\boldsymbol{G}(\boldsymbol{x}(l_0))$ or in other manners. Explicit formulae for the operator $\boldsymbol{G}$ can be found in [3].

The forward extrapolation (10) (deterministic propagation) can be obtained in any MC code by launching *one* particle only and switching off the multiple scattering and the random effects of discrete energy loss due to ionization and delta ray production ("Landau" fluctuations, bremsstrahlung, etc.). What is missing in this procedure is the backward mode and the 5×5 covariance matrix calculation containing the uncertainties of the extrapolation. This is exactly what the track follower has to do.

The elements of the covariance matrix are given by (see tab. 3 for the meaning of the symbols):

$$\sigma_{ij}^2(l) = \left\langle \left(X^i(l) - f^i(l)\right) \left(X^j(l) - f^j(l)\right) \right\rangle \ , \tag{11}$$

where X^i $(i = 1, 2, \ldots, 5)$ indicates the *random* track parameters.

The main task of track following is to calculate the evolution of σ_{ij}^2, that is the error propagation. If the particle is propagated from a track length l_0

to l in a deterministic way, without any random process, then the propagation from a track length l_0 to l can be considered as a function $\boldsymbol{e}[\boldsymbol{f}(l)]$ and described by the transport or Jacobian matrix [1, 5, 6]

$$T_{ij}(l, l_0) = \frac{\partial e^i(l)}{\partial e^j(l_0)} \ . \tag{12}$$

The name of T is due to the property to transport the errors from a track point l_0 to a point l:

$$\delta\boldsymbol{e}(l) = \boldsymbol{T}(l, l_0)\, \delta\boldsymbol{e}(l_0) \ , \tag{13}$$

The error propagation is then obtained with the standard fundamental formula:

$$\boldsymbol{\sigma}^2(l) = \boldsymbol{T}(l, l_0)\, \boldsymbol{\sigma}^2(l_0)\, \boldsymbol{T}^T(l, l_0) + \boldsymbol{W}^{-1}(l) \ , \tag{14}$$

where the first term is the propagation to l of the errors up to l_0 and the second one contains the effects induced by the random processes between l and l_0 (energy loss and multiple scattering) described by the weight matrix $\boldsymbol{W}$. In the covariance matrix $\sigma(l_0)$ are included the multiple scattering and energy loss effects before l_0 and also the measurement errors if the extrapolation starts from the measured points $\boldsymbol{x}$.

The geometrical properties of the transport matrix imply the following equation:

$$\boldsymbol{T}(l_3, l_1) = \boldsymbol{T}(l_3, l_2)\, \boldsymbol{T}(l_2, l_1) \tag{15}$$

If we track in the opposite direction (from l to l_0) along the same trajectory, then

$$\boldsymbol{T}(l_0, l) = \boldsymbol{T}(l, l_0)^{-1} \ . \tag{16}$$

The most common applications of the track following codes are [1, 4]:

- trajectory calculation:
  this is simply the track extrapolation in terms of mean values $\boldsymbol{G}(l)$ and covariance matrix $\boldsymbol{\sigma}$;

- joining track elements:
  to find the best estimate of the intersection $\boldsymbol{x}$ of a particle track in a plane, starting from the measured points (see Fig. 4a)), one can minimize w.r.t. $\boldsymbol{x}$ the χ^2

$$\chi^2(\boldsymbol{x}) = (\boldsymbol{x} - \boldsymbol{G}(l_1))\boldsymbol{W}_1(\boldsymbol{x} - \boldsymbol{G}(l_1))^T + (\boldsymbol{x} - \boldsymbol{G}(l_2))\boldsymbol{W}_2(\boldsymbol{x} - \boldsymbol{G}(l_2))^T \ , \tag{17}$$

obtaining the $\boldsymbol{x}$ estimation as the weighted mean with error

$$\boldsymbol{x} = \frac{\boldsymbol{W}_1\,\boldsymbol{G}(l_1) + \boldsymbol{W}_2\,\boldsymbol{G}(l_2)}{\boldsymbol{W}_1 + \boldsymbol{W}_2} \tag{18}$$

$$\boldsymbol{\sigma}(\boldsymbol{x}) = (\boldsymbol{W}_1 + \boldsymbol{W}_2)^{-1/2}\ ; \tag{19}$$

- track point (vertex) optimization:
  in this case one starts from a track point $\boldsymbol{x}_0$ and finds the best $\boldsymbol{x}_0$ that minimizes the χ^2 up to a track length l_0 (see Fig. 4b)):

$$\chi^2(\boldsymbol{x}_0) = \sum_i \left[(\boldsymbol{x}_i - \boldsymbol{G}(l_i))\,[\boldsymbol{\sigma}^2_{iT}]^{-1}\,(\boldsymbol{x}_i - \boldsymbol{G}(l_i))^T\right]\ , \tag{20}$$

$$\boldsymbol{\sigma}_T = \boldsymbol{\sigma}^2 + \boldsymbol{\sigma}^2_m\ ,$$

  where $\boldsymbol{\sigma}$ and $\boldsymbol{\sigma}_m$ are the extrapolation and measurement covariance matrices respectively, $\boldsymbol{x}_i$ are the track measured points and l_i the track lengths up to $\boldsymbol{x}_i$. The minimization can be done also on a subset of the 5 track parameters [4];

- track fitting with recursive methods:
  the application to Kalman filter will be discussed in detail in sect. 10.

4 The mathematics of track following

The main task here is to find the different contributions which lead to the determination of the error in a point of track length l', starting from a point with a track length $l \neq l'$. The discussion is based mainly on the results reported in [2, 3].

We consider the error propagation along a short length dl from l to $(l + \mathrm{d}l)$. Let $(\delta\boldsymbol{x})_l$ be the variation at l along the track, then the variation at $(l + \mathrm{d}l)$ will be the result of the following contributions:

$$(\delta\boldsymbol{x})_{l+dl} = \underbrace{[(\delta\boldsymbol{x})_l + \mathrm{d}l \cdot A_{l+dl} \cdot (\delta\boldsymbol{x})_l] + \mathrm{d}l \cdot B_{l+dl} \cdot (\delta\boldsymbol{x})_l}_{F_{l+dl}} + (\delta\boldsymbol{x}^M)_{l+dl} \tag{21}$$

The error $(\delta\boldsymbol{x})_{l+dl}$ is composed by:

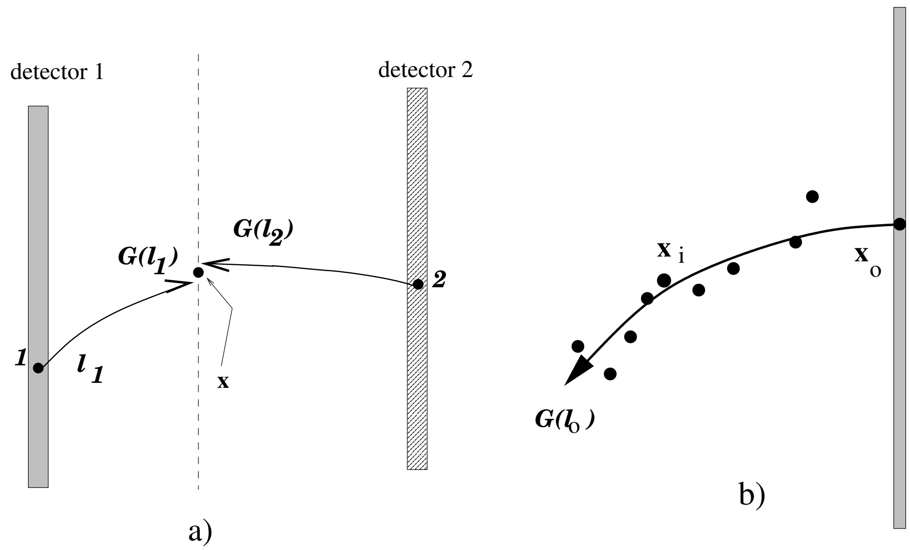

Figure 4: Joining track elements a) and track point optimization b) using a track follower $\boldsymbol{G}(\cdot)$.

- $[(\delta \boldsymbol{x})_l + \mathrm{d}l \cdot A_{l+dl} \cdot (\delta \boldsymbol{x})_l]$, which would be present even without magnetic field and without multiple scattering. The matrix A propagates an error in the direction of the track at l to an error in the position of the track at $(l + \mathrm{d}l)$ (see sect. 5).
- $\mathrm{d}l \cdot B_{l+dl} \cdot (\delta \boldsymbol{x})_l$, which is due to the deflection caused by the magnetic field (see again section 5).
- $(\delta \boldsymbol{x}^M)_{l+dl}$, which is the error due to multiple scattering and energy loss straggling in the interval $(l, l + \mathrm{d}l)$.

By knowing the solution of the infinitesimal displacement given by eq. (21), by dividing the total length of the track L into n small steps of size $\mathrm{d}l = L/n$ and applying the above relation for each step one obtains [2]

$$(\delta \boldsymbol{x})_L = (\prod_{j=n}^{1} \boldsymbol{F}_j)(\delta \boldsymbol{x})_0 + \sum_{v=1}^{n-1} [(\prod_{j=n}^{v+1} \boldsymbol{F}_j) \cdot (\delta \boldsymbol{x}^M)_v] + (\delta \boldsymbol{x}^M)_n \tag{22}$$

Detailed calculations can be found in Appendix A.

The connection between F and the Jacobian is

$$\boldsymbol{T}(l_2, l_1) = \lim_{dl \to 0} \left(\prod_{j=\mu_2}^{\mu_1} \boldsymbol{F}_j \right) . \tag{23}$$

The matrices $\boldsymbol{F}_j$ may be calculated step by step during the track following and equation (23) thus gives the full error propagation from l_1 to l_2 without further approximations.

Since there is no correlation between the multiple scattering and energy loss variations $(\delta \boldsymbol{x}^M)_{l+dl}$ in two different points of the track, their contribution is usually calculated as a random component in the covariance (error) matrix and included in the matrix $\boldsymbol{W}^{-1}$ in eq. (14) step by step (see sects. 6, 7). In a current step, the random error from the previous step is included in $\boldsymbol{\sigma}^2$ of eq. (14) and propagated with the Jacobian. This is also the procedure followed by GEANE [4].

Therefore, we can omit the $(\delta \boldsymbol{x}^M)_{l+dl}$ term in eq. (22) and write the correspondence between the matrix $\boldsymbol{F}$ and the transport matrix of eq. (13) as:

$$\boldsymbol{T}(l + \mathrm{d}l, l) = \boldsymbol{F} = \boldsymbol{I} + (\boldsymbol{A}_{l+dl} + \boldsymbol{B}_{l+dl}) \cdot \mathrm{d}l \ , \tag{24}$$

which represents the error propgation in an elementary tracking step.

In the next sections we will give the explicit expressions for these matrices, in the form used by GEANE. Their insertion in eq. (14) will give the Jacobian for the covariance matrix transformation.

5 The basic Jacobian

In this section we collect the complicated formulae to solve eqs. (21, 24), that can be used if one wants to write new codes in alternative or in addition to the existing ones. The differential and the variation (uncertainty) on any quantity x will be denoted as $\mathrm{d}x$ and δx, respectively. The uncertainties will be considered as small variations of the quantity of interest.

We consider the SC system, where the infinitesimal spatial displacements of the particle after a track length l can be denoted as $\mathrm{d}y_\perp$ and $\mathrm{d}z_\perp$, whereas those on the track direction as $\mathrm{d}\lambda$ and $\mathrm{d}\phi$. $\mathrm{d}z_\perp$ lies on the $(z_\perp, x_\perp)$ plane and corresponds to a rotation around the $y_\perp$ axis, $\mathrm{d}y_\perp$ lies on the $(x_\perp, y_\perp)$ plane and refers to a rotation around the $z_\perp$ axis. From fig. 5 one sees that

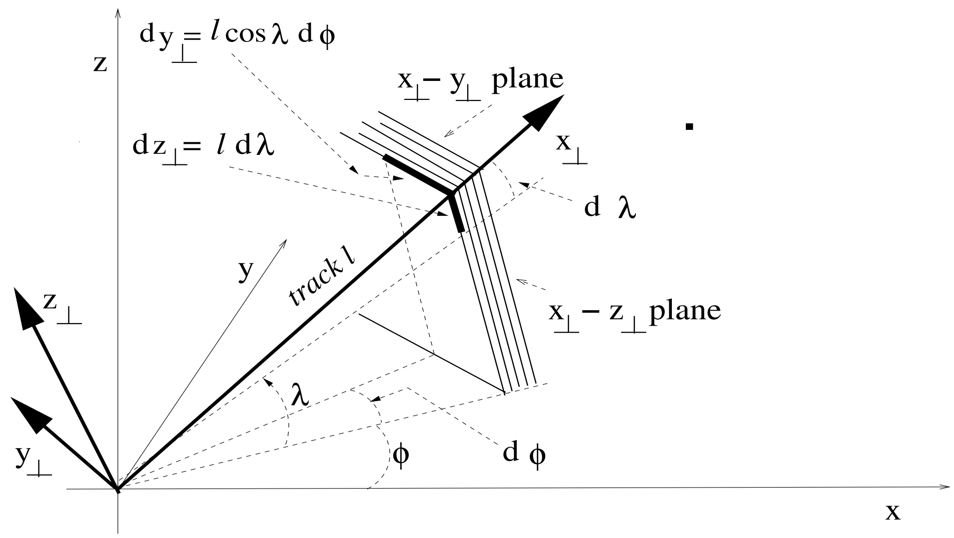

Figure 5: The connection between small deflections $\mathrm{d}\lambda$ and $\mathrm{d}\phi$ and the displacements $\mathrm{d}y_\perp$, $\mathrm{d}z_\perp$ in the transverse SC system $(1/p, \lambda, \phi, x_\perp, y_\perp, z_\perp)$. Recall that $x_\perp$ is along the unscattered track and that $y_\perp$ lies on the $x-y$ plane.

these deviations are connected each other by the equations:

$$\mathrm{d}z_\perp = l\ \mathrm{d}\lambda\ , \qquad \mathrm{d}y_\perp = l\ \cos\lambda\,\mathrm{d}\phi\ , \tag{25}$$

One obtains, with the help of the equations above, the transformation between two transverse SC systems which are related to each other by an infinitesimal track rotation

$$\mathrm{d}\beta = -\,\mathrm{d}z_\perp/l = -\,\mathrm{d}\lambda\ , \qquad \mathrm{d}\gamma = \mathrm{d}y_\perp/l = \cos\lambda\ \mathrm{d}\phi$$

around the $y_\perp$ and $z_\perp$ axes, respectively (for the calculations see Appendix A):

$$\begin{pmatrix} x'_\perp \\ y'_\perp \\ z'_\perp \end{pmatrix} = \begin{pmatrix} 1 & \mathrm{d}\gamma & -\,\mathrm{d}\beta \\ -\,\mathrm{d}\gamma & 1 & \tan\lambda\,\mathrm{d}\gamma \\ \mathrm{d}\beta & -\tan\lambda\,\mathrm{d}\gamma & 1 \end{pmatrix} \begin{pmatrix} x_\perp \\ y_\perp \\ z_\perp \end{pmatrix} \tag{26}$$

where the minus sign between β and λ is due to the opposite orientation between the polar and the dip angle.

From this matrix one sees that the rotations $\mathrm{d}\gamma$, $\mathrm{d}\beta$ imply, due to the definition of the transverse reference frame, also a rotation around the $x_\perp$ axis by an angle $\mathrm{d}\alpha = \tan\lambda\ \mathrm{d}\gamma$.

In terms of the SC variables, where λ and ϕ are defined in MARS, with the help of eqs. (25), eq. (26) reads:

$$\begin{pmatrix} x'_\perp \\ y'_\perp \\ z'_\perp \end{pmatrix} = \begin{pmatrix} 1 & \cos\lambda\,\mathrm{d}\phi & \mathrm{d}\lambda \\ -\cos\lambda\,\mathrm{d}\phi & 1 & \sin\lambda\,\mathrm{d}\phi \\ -\mathrm{d}\lambda & -\sin\lambda\,\mathrm{d}\phi & 1 \end{pmatrix} \begin{pmatrix} x_\perp \\ y_\perp \\ z_\perp \end{pmatrix} \tag{27}$$

The infinitesimal transformation (27) defines the following rotation vector:

$$\mathrm{d}\boldsymbol{\theta} = \begin{pmatrix} \text{rotation around } x_\perp \\ \text{rotation around } y_\perp \\ \text{rotation around } z_\perp \end{pmatrix} = \begin{pmatrix} \sin\lambda\ \mathrm{d}\phi \\ -\mathrm{d}\lambda \\ \cos\lambda\ \mathrm{d}\phi \end{pmatrix} \tag{28}$$

Now we have to find the matrix elements of

$$\boldsymbol{F} = \boldsymbol{I} + (\boldsymbol{A}_{l+dl} + \boldsymbol{B}_{l+dl}) \cdot \mathrm{d}l = \frac{\partial \boldsymbol{e}_{l+dl}}{\partial \boldsymbol{e}_l}\ , \tag{29}$$

where $\boldsymbol{e}$ is the track defined in the SC system.

The multiple scattering effects will be considered in sect. 6, the energy loss ones, that add a random noise variance $\sigma^2_{11}(l)$ in eq. (14), will be discussed in sect.7.

Firstly, we consider the matrix $\boldsymbol{A}_{l+dl} \cdot \mathrm{d}l$, which propagates the errors without taking into account the magnetic field. In this case the track runs along a straight line and the derivatives involving λ and ϕ are zero. The non zero terms are due to the uncertainties in the position $\delta y_\perp$ and $\delta z_\perp$ at l which propagates linearly at $l + \mathrm{d}l$ on some track variables. They affect:

1. the momentum $1/p$. This uncertainty arises from the mean energy loss calculation, which depends on the thickness traversed: any uncertainty in $\delta(1/p)_l$ due to an uncertainty $\delta(\,\mathrm{d}l)$ will change while decreasing the momentum. Note that this uncertainty is different from the energy straggling, which is the dispersion around the mean value and that will be treated in sect. 7. For this error one finds (for a detailed derivation see Appendix C):

$$\delta\left(\frac{1}{p}\right)_{l+dl} = \left[\frac{\left(\frac{d\frac{1}{p}}{dl}\right)_{l+dl}}{\left(\frac{d\frac{1}{p}}{dl}\right)_l}\right]\delta\left(\frac{1}{p}\right)_l$$

$$= \quad \left[1 + \frac{\left(\frac{d^2 \frac{1}{p}}{dl^2}\right)}{\left(\frac{d \frac{1}{p}}{dl}\right)} \cdot \mathrm{d}l\right] \delta\left(\frac{1}{p}\right)_l \tag{30}$$

2. from the first of eqs. (25), where in this case $l \equiv \mathrm{d}l$ and the small uncertainties are approximated as differentials, one has

$$\boldsymbol{A}_{l+dl}(5,2) \cdot \mathrm{d}l = \frac{\partial z_\perp}{\partial \lambda} = \mathrm{d}l \ ;$$

3. from the second of eqs. (25) one has

$$\boldsymbol{A}_{l+dl}(4,3) \cdot \mathrm{d}l = \frac{\partial y_\perp}{\partial \phi} = \cos\lambda \ \mathrm{d}l \ ;$$

In summary, for the term $\boldsymbol{I} + \boldsymbol{A}_{l+dl} \cdot \mathrm{d}l$ we have obtained:

$$\begin{pmatrix} \delta(1/p) \\ \delta\lambda \\ \delta\phi \\ \delta y_\perp \\ \delta z_\perp \end{pmatrix}_{l+dl} = \begin{pmatrix} 1 + \frac{\left(\frac{d^2 \frac{1}{p}}{dl^2}\right)}{\left(\frac{d \frac{1}{p}}{dl}\right)} \cdot \mathrm{d}l & 0 & 0 & 0 & 0 \\ 0 & 1 & 0 & 0 & 0 \\ 0 & 0 & 1 & 0 & 0 \\ 0 & 0 & \cos\lambda \ \mathrm{d}l & 1 & 0 \\ 0 & 1 & 0 & 0 & 1 \end{pmatrix} \begin{pmatrix} \delta(1/p) \\ \delta\lambda \\ \delta\phi \\ \delta y_\perp \\ \delta z_\perp \end{pmatrix}_l$$

From this, matrix A follows:

$$\boldsymbol{A} = \begin{pmatrix} \frac{\left(\frac{\partial^2 1/p}{\partial l^2}\right)}{\left(\frac{\partial 1/p}{\partial l}\right)} & 0 & 0 & 0 & 0 \\ 0 & 0 & 0 & 0 & 0 \\ 0 & 0 & 0 & 0 & 0 \\ 0 & 0 & \cos\lambda & 0 & 0 \\ 0 & 1 & 0 & 0 & 0 \end{pmatrix} \tag{31}$$

Now we consider the matrix B.

In this case we have to consider the effects of the deflections due to the magnetic field B. The key relations are the Lorentz force and the helix equation for a particle of momentum p and charge q. When the field is along the z axis and the trajectory lies in the x-y plane, these equations become:

$$\left\{ \begin{array}{lcl} p & = & qRB \equiv -HR \\ \mathrm{d}l & = & R\,\mathrm{d}\phi \end{array} \right. \quad \rightarrow \quad \mathrm{d}\phi = -H\frac{\mathrm{d}l}{p} \ , \tag{32}$$

where in the last passage the curvature radius R has been eliminated and $H = \pm 0.3 \cdot 10^{-3}$ GeV/(cm kG) qB; the sign refers to negative or positive charged particles, respectively.

Now we have to generalize the equation above in the SC system for any orientation field-particle momentum. To this end we consider the field $\boldsymbol{H} = (H_1, H_2, H_3)$ in the SC system and apply, for any component, eq. (32). The azimuthal angle ϕ transforms in the rotation vector (28) and we have:

$$\mathrm{d}\boldsymbol{\theta} = -\boldsymbol{H}\frac{\mathrm{d}l}{p} = -\begin{pmatrix} H_1/p \\ H_2/p \\ H_3/p \end{pmatrix} \cdot \mathrm{d}l = \begin{pmatrix} \mathrm{d}\alpha \\ \mathrm{d}\beta \\ \mathrm{d}\gamma \end{pmatrix} = \begin{pmatrix} \sin\lambda\ \mathrm{d}\phi \\ -\,\mathrm{d}\lambda \\ \cos\lambda\ \mathrm{d}\phi \end{pmatrix} \ . \tag{33}$$

Note that $|\,\mathrm{d}\theta|^2 = \mathrm{d}\lambda^2 + \mathrm{d}\phi^2$ as shown in fig.6

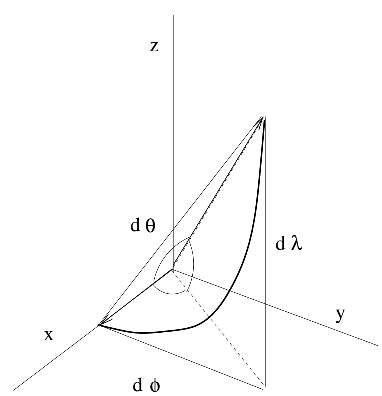

Figure 6: The geometry of the helix in the MARS system. The analog in the SC system is eq. (33).

Eq. (33) means that the momentum vector of the particle with momentum p is rotated by a magnetic field $\boldsymbol{H}$ over a track length $\mathrm{d}l$ by an angle $\mathrm{d}\theta$ with rotation axis parallel or antiparallel to $\boldsymbol{H}$.

To transform the magnetic field components $H = (H_x, H_y, H_z)$ measured in the MARS system to the components $H = (H_1, H_2, H_3)$ the the SC system, one has to apply eq. (9). For a detailed calculation see Appendix D:

$$\begin{array}{rcrcrcr} H_0 & = & H_x \cos\phi & + & H_y \sin\phi & = & -\,\mathrm{d}H_2/\,\mathrm{d}\phi \\ H_1 & = & H_0 \cos\lambda & + & H_z \sin\lambda & = & -\,\mathrm{d}H_3/\,\mathrm{d}\lambda \\ H_2 & = & -H_x \sin\phi & + & H_y \cos\phi & = & \mathrm{d}H_0/\,\mathrm{d}\phi \\ H_3 & = & -H_0 \sin\lambda & + & H_z \cos\lambda & = & \mathrm{d}H_1/\,\mathrm{d}\lambda \end{array} \tag{34}$$

Now from eq. (33) we obtain:

$$\begin{pmatrix} \mathrm{d}\lambda \\ \mathrm{d}\phi \end{pmatrix} = -\frac{\mathrm{d}l}{p} \begin{pmatrix} -H_2 \\ H_3/\cos\lambda \end{pmatrix} \tag{35}$$

After this passage, we finally are able to calculate all the derivatives of the matrix B by using eq.(29). The track parameter variations are calculated at first order:

$$\delta(e_j)_{l+dl} = \sum_i \frac{\partial e_j}{\partial e_i}\,\delta(e_i)_l\ , \quad \text{where} \ \ \boldsymbol{e} = [1/p, \lambda, \phi, y_\perp, z_\perp]\ . \tag{36}$$

For the angles, from eqs. (35, 36) we have:

$$\delta \begin{pmatrix} \mathrm{d}\lambda \\ \mathrm{d}\phi \end{pmatrix}_{l+dl} = -\begin{pmatrix} -H_2 \\ \dfrac{H_3}{\cos\lambda} \end{pmatrix} \mathrm{d}l \cdot \delta(1/p)_l - \frac{1}{p} \begin{pmatrix} -H_2 \\ \dfrac{H_3}{\cos\lambda} \end{pmatrix} \delta(\,\mathrm{d}l) - \frac{\mathrm{d}l}{p} \cdot \delta \begin{pmatrix} -H_2 \\ \dfrac{H_3}{\cos\lambda} \end{pmatrix}\ . \tag{37}$$

Here the term $\delta(\,\mathrm{d}l)$ appears that has to be calculated explicitly. Since in the SC system the $x_\perp$ coordinate is a known parameter that defines the transverse plane, we have $\delta(x_\perp) = 0$. This constraint usually implies $\delta(\,\mathrm{d}l) \neq 0$ (see fig. 7), and this uncertainty has to be assigned to $x_\perp$, since $y_\perp$ and $z_\perp$ lie on the plane $x_\perp = $ const. transverse to the track direction. At l then we have:

$$\begin{pmatrix} \delta x_\perp \\ \delta y_\perp \\ \delta z_\perp \end{pmatrix}_l = \begin{pmatrix} 0 \\ \delta y_\perp \\ \delta z_\perp \end{pmatrix}_l\ . \tag{38}$$

Therefore, by using eq. (27), in the SC system the spatial variation must be written as:

$$\begin{pmatrix} 0 \\ \delta y_\perp \\ \delta z_\perp \end{pmatrix}_{l+dl} = \begin{pmatrix} 1 & \cos\lambda\,\mathrm{d}\phi & \mathrm{d}\lambda \\ -\cos\lambda\,\mathrm{d}\phi & 1 & \sin\lambda\,\mathrm{d}\phi \\ -\,\mathrm{d}\lambda & -\sin\lambda\,\mathrm{d}\phi & 1 \end{pmatrix} \begin{pmatrix} 0 \\ \delta y_\perp \\ \delta z_\perp \end{pmatrix}_l + \begin{pmatrix} \delta(dl) \\ 0 \\ 0 \end{pmatrix} \tag{39}$$

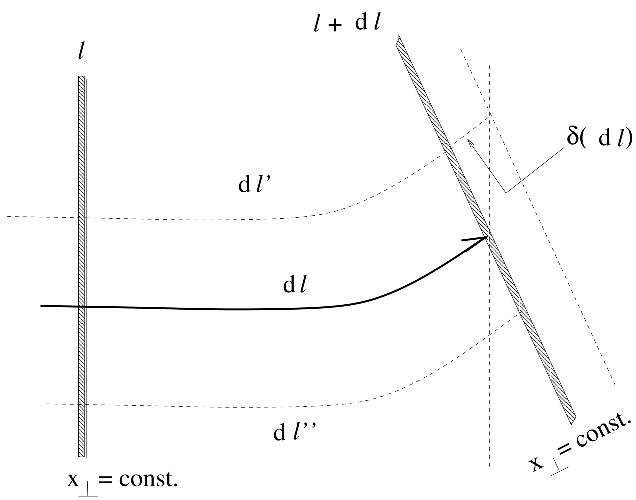

Figure 7: The tracking in the SC system: the curvature effect of the magnetic field gives $\delta(\,\mathrm{d}l) \neq 0$.

The first row of eq. (39) gives the required relation for $\delta(\,\mathrm{d}l)$:

$$\begin{aligned} \delta(\,\mathrm{d}l) &= -\cos\lambda\ \mathrm{d}\phi \cdot \delta(y_\perp)_l - \ \mathrm{d}\lambda \cdot \delta(z_\perp)_l \\ &= \frac{H_3}{p}\ \mathrm{d}l \cdot \delta(y_\perp)_l - \frac{H_2}{p}\,\mathrm{d}l \cdot \delta(z_\perp)_l\ , \end{aligned} \tag{40}$$

where the last member, which contains only the differential $\mathrm{d}l$ as required, is deduced from eq. (33).

The last step is to develop the apparent variation of the magnetic field due to the parameter uncertainties, that is the last term of eq (37). By differentiating eqs. (34) according to eq. (29) one obtains (see Appendix E):

$$\delta \begin{pmatrix} -H_2 \\ H_3/\cos\lambda \end{pmatrix}_l = \begin{pmatrix} 0 \\ -H_0/\cos^2\lambda \end{pmatrix} \delta(\lambda)_l + \begin{pmatrix} H_0 \\ -\tan\lambda\, H_2 \end{pmatrix} \delta(\phi)_l \tag{41}$$

From eqs. (26, 29, 33, 35, 37, 39, 40, 41) one finally obtains the desired form of the B matrix:

$$B = \begin{pmatrix} 0 & 0 & 0 & 0 & 0 \\ H_2 & 0 & -H_0/p & H_2H_3/p^2 & -H_2^2/p^2 \\ -\dfrac{H_3}{\cos\lambda} & \dfrac{H_0}{p\cos^2\lambda} & \dfrac{H_2\tan\lambda}{p} & -\dfrac{H_3^2}{p^2\cos\lambda} & \dfrac{H_2H_3}{p^2\cos\lambda} \\ 0 & 0 & 0 & 0 & -\dfrac{H_3\tan\lambda}{p} \\ 0 & 0 & 0 & \dfrac{H_3\tan\lambda}{p} & 0 \end{pmatrix} \tag{42}$$

For example, the term in the fourth row is obtained from eq. (33) in the following way:

$$\begin{aligned} \delta(y_\perp)_{l+dl} &= \delta(y_\perp)_l + \sin\lambda\, \mathrm{d}\phi\, \delta(z_\perp)_l = \delta(y_\perp)_l - \frac{\sin\lambda H_3\ \mathrm{d}l}{\cos\lambda\, p}\, \delta(z_\perp)_l \\ &= \delta(y_\perp)_l - \frac{H_3\tan\lambda}{p}\ \mathrm{d}l\, \delta(z_\perp)_l \end{aligned}$$

and hence, from eq. (36):

$$B_{4,5} = \frac{\partial(y_\perp)_{l+dl}}{\partial(z_\perp)_l} = -\frac{H_3\ \tan\lambda}{p}\ \mathrm{d}l\ ,$$

where eqs. (33, 39) have been used.

The matrices deduced in this section are calculated by the GEANE routine TRPROP. In this routine the energy loss term $A(1,1)$ in eq. (31) is not considered.

By using the option 'E' in ERTRAK, the routine TRPRFN is called in alternative, which calculates the propagation in a finite step length assuming an exact helix trajectory. However, this option should not be used in a realistic case.

6 Multiple scattering effects

The two quantities of interest in the multiple scattering process are the displacement Δ and the scattering angle θ. The theory of Molière, that finds the statistical distribution of θ is reviewed in [10] (we refer the reader to the references therein for an essential bibliography). The distribution can be approximated as the sum of two gaussians, a core one that takes into account the bulk process and a flat one that describes the tails.

In the small angle approximation, it is more convenient to work in term of projected scattering angles. If the particle runs along the z-axis, the deflection θ can be represented as a segment in the $x-y$ plane where $\theta_x = \theta\cos\phi$, $\theta_y = \theta\sin\phi$ and $\theta^2 = \theta_x^2 + \theta_y^2$ (see fig. 8).

In a plane, the two quantities of interest in the multiple scattering process are then the displacement x and the *projected* scattering angle $\theta_p \equiv \theta_x = \theta_y$ (see fig. 8). The θ_p total projected *variance* for a particle of momentum p (in

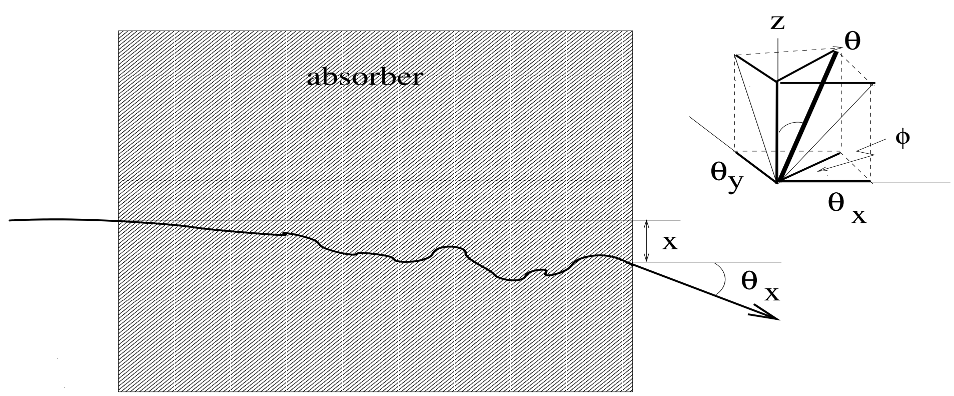

Figure 8: The multiple scattering angle θ_x and the displacement x through an absorber.

GeV/c) that travels through an absorber of thickness d is expressed as [10]:

$$< \theta_p^2 >= \frac{225 \cdot 10^{-6}}{p^2} \frac{d}{\beta^2 X_s} , \qquad X_s = X_0 \frac{Z+1}{Z} \frac{\ln(287\, Z^{-1/2})}{\ln(159\, Z^{-1/3})} \qquad (43)$$

where X_0 is the radiation length of the absorber.

The standard practice is to parametrize the core variance as [11]:

$$< \theta_p^2 >= \frac{(0.0136)^2\, d}{p^2\, \beta^2 X_0} \left[1 + 0.038\, \ln\left(\frac{d}{X_0}\right)\right]^2 \qquad (44)$$

However, this variance should not be used in track following for two reasons:

1. it is not the whole variance, so that the pull quantities show an underestimation of the multiple scattering errors;

2. the thickness contained in the logarithmic term makes the calculation dependent on the tracking steps. Indeed, to make the calculation independent of the layers in which an absorber is divided, the variance should be directly proportional to the thickness d, as in (43).

Hence, we emphasize that the variance (43) should be used, which is the result of the accurate treatment of [10]. In this case, slight deviations from the gaussian form of the pull distribution have to be expected, since the angle distribution has non gaussian tails.

In GEANE the following formula is used:

$$< \theta_p^2 >= \frac{184.96 \cdot 10^{-6}}{p^2} \frac{d}{\beta^2 X_0} \ . \tag{45}$$

We substituted this formula with eq. (43). The results improve only slightly the pull distribution $(\lambda_{\text{GEANE}} - \lambda_{\text{true}})/\sigma_{\text{GEANE}}$ of the dip angle (fig. 9) since, for most light scatterers, the ratio $X_s/X_0 \simeq 1.15$ is near to the ratio $225/185 = 1.21$ [10].

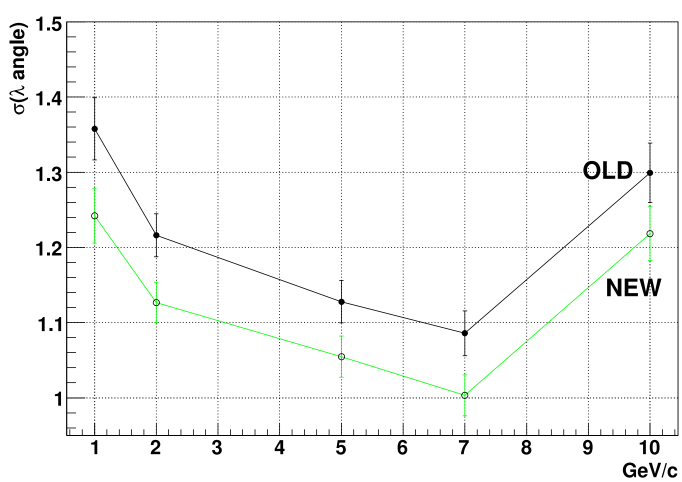

Figure 9: Behaviour with energy of the σ of the pull distribution of the dip angle λ. OLD with eq. (45), NEW with eq. (43).

The multiple scattering treatment in track following codes is based on the joint probability distribution of the lateral displacement x and of the projected angle θ_p for an absorber of thickness d. This distribution, that probably goes back to Fermi, is deduced in the famous old book of Rossi [12]:

$$p(x, \theta_p; d) = \frac{2\sqrt{3}}{\pi} \frac{1}{< \theta_p^2 > d^2} \exp\left[-\frac{4}{< \theta_p^2 >} \left(\frac{\theta_p^2}{d} - \frac{3x\theta_p}{d^2} + \frac{3x^2}{d^3} \right) \right]$$

From this distribution it is straightforward to obtain the following variances and covariances [1, 11]:

$$< \theta_p^2 > , \quad < x^2 >= \frac{< \theta_p^2 > \; d^2}{3} , \qquad < x, \theta_p >= \frac{< \theta_p^2 > \; d}{2} \tag{46}$$

In a tracking problem, the naive multiple scattering variables for a particle running along the x-axis making *small* angular and lateral deviations are:

$$s_i = [0, \; y, \; \theta_y, \; z, \; \theta_z] \; , \tag{47}$$

where the five positions are considered for compatibility with the track formalism. GEANE treats multiple scattering effects in the SC system

$$t_i = [1/p, \; \lambda, \; \phi, \; y_\perp, \; z_\perp] \; , \tag{48}$$

which is the most natural one in this case. The transport in the SD system, when necessary, is made through the internal service routines of the code. From eq. (25), and considering that the angles θ_z, θ_y are small, one finds the following correspondence:

$$\lambda \equiv -\theta_z \; , \quad \phi \equiv \frac{\theta_y}{\cos\lambda} \; , \quad y_\perp \equiv y \; , \quad z_\perp \equiv z \; . \tag{49}$$

Note that in these formulas $\cos\lambda$, which is the track angle before the multiple scattering act, is simply a parameter. In what follows, the projected angles $\theta_y = \theta_z = \theta_p$ are supposed uncorrelated, that is $< \theta_y, \theta_z >= 0$ (although uncorrelated, they are not independent! [10]).

To transport the errors from the multiple scattering reference to SC, we use the standard error propagation [13]:

$$< t_i, t_j >= \sum_{lm} \frac{\partial t_i}{\partial s_l} \frac{\partial t_j}{\partial s_m} < s_l, s_m > \; . \tag{50}$$

Taking into account (46, 47-49) and writing only non-zero terms, we easily obtain the elements of the multiple scattering covariance matrix in the SC system [1]:

$$
\begin{aligned}
<\lambda^2> &= <\theta_z^2>=<\theta_p^2>\,, && (51)\\
<\lambda, z> &= -<\theta_p, z>=-\frac{<\theta_p^2>\ d}{2}\,, && (52)\\
<\phi^2> &= \frac{<\theta_p^2>}{\cos^2\lambda}\,, && (53)\\
<y,\phi> &= \frac{\partial y}{\partial y}\frac{\partial \phi}{\partial \theta_y}<y,\theta_y>=\frac{1}{\cos\lambda}\frac{<\theta_p^2>\ d}{2} && (54)\\
<y^2> &= \frac{<\theta_p^2>\ d^2}{3} && (55)\\
<z^2> &= \frac{<\theta_p^2>\ d^2}{3} && (56)
\end{aligned}
$$

The transport of the multiple scattering errors is then given by the symmetric matrix $\boldsymbol{W}^{-1}$ in eq. (14). Since in the track transport formalism the thickness corresponds to the tracking step, $d \equiv \mathrm{d}l$, the final form of $\boldsymbol{W}^{-1}$ in the SC variables $1/p$, λ, ϕ, $y_\perp$, $z_\perp$ is

$$
\begin{pmatrix}
0 & 0 & 0 & 0 & 0\\
0 & <\theta_p^2> & 0 & 0 & -\frac{<\theta_p^2>\ \mathrm{d}l}{2}\\
0 & 0 & \frac{<\theta_p^2>}{\cos^2\lambda} & \frac{<\theta_p^2>\ \mathrm{d}l}{(2\cos\lambda)} & 0\\
0 & 0 & \frac{<\theta_p^2>\ \mathrm{d}l}{(2\cos\lambda)} & \frac{<\theta_p^2>\ (\mathrm{d}l)^2}{3} & \\
0 & -\frac{<\theta_p^2>\ \mathrm{d}l}{2} & 0 & 0 & \frac{<\theta_p^2>\ (\mathrm{d}l)^2}{3}
\end{pmatrix} \qquad (57)
$$

This is the matrix used by GEANE (routine ERMCSC). In the version for PANDA, we use eq. (43) instead of eq. (45) for $<\theta_p^2>$.

7 Energy loss fluctuations

The fluctuations in ionization for one particle of charge z, mass m, velocity β, are characterized by the parameter κ,

$$\kappa = \frac{\xi}{E_{\max}} \ , \tag{58}$$

which is proportional to the ratio of mean energy loss to the maximum allowed energy transfer $E_{\max}$ in a single collision with an atomic electron:

$$E_{\max} = \frac{2 m_e \beta^2 \gamma^2}{1 + 2\gamma m_e/m + (m_e/m)^2} \ , \tag{59}$$

where $\gamma = 1/\sqrt{1-\beta^2} = E/m$ and m_e is the electron mass. The parameter ξ comes from the Rutherford scattering cross section and is defined as [11]:

$$\xi = 153.4 \frac{z^2 Z}{\beta^2 A} \rho d \quad (\mathrm{keV}) \ , \tag{60}$$

where ρ, d, Z and A are the density (g/cm^3), thickness, atomic and mass number of the medium.

The parameter κ takes into account both the projectile energy and the geometrical thickness of the absorber; it defines univocally the absorber characteristics, that is the straggling conditions [15]:

1. for heavy absorbers, $\kappa > 10$ and the distribution is gaussian;
2. for moderate absorbers, $0.01 < \kappa < 10$ and the distribution follows the function of Vavilov [15], that tends smoothly to the gaussian by increasing the thickness;
3. when $\kappa < 0.01$, we are in the presence of thin absorbers. When the number of collisions $N_c > 50$, the distribution follows the Landau function [15];
4. for very thin absorbers, $N_c < 50$ (the condition $\kappa \ll 0.01$ is implicitly fulfilled) and there are no universal straggling functions, but only approximated models [14]. We will call this as the *sub-Landau* condition or regime; it is the dominant one in gaseous detectors at PANDA energies.

$\lambda_{\max}$	α	Mean	σ_α
11.1	0.90	1.61	2.83
22.4	0.95	2.40	4.23
110.0	0.99	4.19	10.16
200.0	0.995	4.82	13.88
256.0	0.996	5.08	15.76
339.0	0.997	5.37	18.19
507.0	0.998	5.78	22.33
1007.0	0.999	6.48	31.59

Table 1: Result of the integration $\alpha = \int_{\lambda_{\min}}^{\lambda_{\max}} f(\lambda)\,\mathrm{d}\lambda$ of the Landau distribution from $\lambda_{\min} \simeq -3.5$ to $\lambda_{\max}$ of the table. The mean and the standard deviation of the truncated distribution are also shown. For this distribution. the full mean and the variance are infinite, only the cumulative can be calculated.

For the cases 1. and 2. the straggling problem has a definite solution, both in simulation and in track following, because the general theory of the moments of the energy straggling distribution, based on the transport equation [9], shows that the energy variance is given by:

$$\sigma^2(E) = \frac{\xi^2}{\kappa}(1-\beta^2/2) = \xi\, E_{\max}(1-\beta^2/2)\ . \tag{61}$$

For the Landau distribution, that assumes $E_{\max} = \infty$, *both the average and the variance are infinite* [1, 13] (see Tab. 1).

Taking into account the energy-momentum equation

$$E^2 = p^2 + m^2 \quad \rightarrow \quad \frac{\mathrm{dp}}{\mathrm{dE}} = \frac{E}{p} = \frac{1}{\beta}\ ,$$

and the error transformation

$$\sigma^2(1/p) = \left[\frac{\mathrm{d}}{\mathrm{dp}}\left(\frac{1}{p}\right)\right]^2 \sigma^2(p) = \frac{1}{p^4}\,\sigma^2(p) = \frac{E^2}{p^6}\,\sigma^2(E)$$

we obtain the variance on $1/p$. This quantity is calculated by GEANE in the routine ERLAND and added to the covariance matrix σ_{11} of eq.(14) in the routine ERPROP at the end of the tracking step:

$$\sigma_{11}^2(l) = \frac{E^2}{p^6}\,\sigma^2(E) = \frac{E^2}{p^6}\,\xi\, E_{\max}(1-\beta^2/2)\ . \tag{62}$$

Since this is the only energy straggling considered, the GEANE results are completely unreliable for thin layers, where the Landau or sub-Landau conditions 3. and 4. often are verified.

To remedy to this situation, we have implemented the PANDA version of GEANE with the procedure explained below, that has been inserted in the old GEANE routine ERLAND.

Firstly, we note that, for thin and very thin absorbers, a rigorous solution exists for the simulation but not for track following. Indeed, whereas in the simulation the sampling and the tracking of the δ-electrons reproduces correctly some rare effects in the detectors or the noise characteristics, in track following the long tail of the energy lost by the particle, due to the δ-electron emission, makes the energy straggling variance infinite (for the Landau distribution [1, 13]) or so big (in sub-Landau models [14]) that the uncertainty in the track momentum is meaningless, because these fluctuations refer to "enormous" energy losses occurring with very low probability.

Since an universally accepted solution of this problem at present does not exists, we use some approximations based on truncated distributions. In the Landau regime we consider the Landau variable

$$\lambda = \frac{E - E_{\rm med}}{\xi} - 1 + \gamma' - \beta^2 - \ln \kappa \tag{63}$$

where $\gamma' = 0.57725$ is the Euler's constant, and we cut the Landau distribution $f_L(\lambda)$ to an area α, corresponding to a value σ_α given by tab 1. Then, from eq. (63), for the Landau case we assume:

$$\sigma(E) = \xi \, \sigma_\alpha \ . \tag{64}$$

For example, for $\alpha = 0.95$ we have, from tab. 1, $\sigma(E) = 4.23\,\xi$.

In the sub-Landau case we have the further difficulty due to the non existence of a straggling density in a closed analytical form [14]. In this case we decided to use a variance value obtained from the Urban model [16], which is one of the models used to sample the energy lost by the particle in very thin absorbers both in GEANT3 and GEANT4 [15].

The Urban model is based on the following formulae [16]:

- excitation macroscopic cross sections Σ_1 and Σ_2:

$$\Sigma_i = C \frac{f_i}{E_i} \frac{\ln(2m\beta^2\gamma^2/e_i) - \beta^2}{\ln(2m\beta^2\gamma^2/I) - \beta^2}(1 - r) \ , \quad i = 1, 2$$

where:

$$I = 16Z^{0.9}\ (\mathrm{eV})\ , \quad f_2 = \begin{cases} 0 \text{ if} Z \leq 2 \\ 2/Z \text{ if} Z > 2 \end{cases} \quad , \quad f_1 = 1 - f_2$$

$$e_2 = 10Z^2\ (\mathrm{eV})\ , \quad e_1 = \left(\frac{I}{e_2^{f_2}}\right)^{1/f_1} \quad , \quad r = 0.4\ , \quad C = \frac{E_{\mathrm{med}}}{\Delta x}\ ,$$

and $E_{\mathrm{med}} \equiv (\mathrm{d}E/\mathrm{d}x) \cdot \Delta x$ is the energy lost in the absorber of thickness Δx;

- ionization macroscopic cross section Σ_3:

$$\Sigma_3 = C\, \frac{E_{\mathrm{max}}}{I(E_{\mathrm{max}} + I)\ln((E_{\mathrm{max}} + I)/I)}\, r$$

- number of total collisions N_c:

$$N_c = (\Sigma_1 + \Sigma_2 + \Sigma_3)\Delta x = N_1 + N_2 + N_3\ . \tag{65}$$

- total energy lost:

$$E = (\Sigma_1 e_1 + \Sigma_2 e_2 + \Sigma_3 E_3)\Delta x = N_1 e_1 + N_2 e_2 + N_3 E_3\ , \tag{66}$$

  where e_1 and e_2 are the two fixed excitation energies of the model and E_3 is the energy lost by δ-electron emission. This is a stochastic quantity that follows approximately the distribution [16]:

$$E_3 \sim g(E) \text{ where } g(E) = \frac{I(E_{\mathrm{max}} + I)}{E_{\mathrm{max}}}\,\frac{1}{E^2}\ , \quad I < E < E_{\mathrm{max}} + I\ . \tag{67}$$

In GEANT3 and GEANT4 the energy E is obtained by eq. (66) by sampling N_1, N_2 and N_3 from the Poisson distribution and E_3 from $g(E)$. This last sampling gives (unlikely) strong fluctuations: for example, for 1 GeV pions in 1 cm Ar we have $E_{\mathrm{med}} \simeq 2.5$ keV, $E_{\mathrm{max}} \simeq 66$ MeV and a standard deviation of about 100 keV due to the δ-electrons tail.

We decided here to truncate the Urban distribution, considering a standard deviation representing a percentage α of the area of the δ-electron energy distribution (67):

$$\frac{I(E_{\mathrm{max}} + I)}{E\mathrm{max}} \int_I^{E_\alpha} \frac{1}{E^2}\,\mathrm{d}E = \frac{(E_{\mathrm{max}} + I)}{E_{\mathrm{max}}}\frac{E_\alpha - I}{E_\alpha} = \alpha$$

$$\rightarrow E_\alpha = \frac{I}{1 - \alpha\, E_{\mathrm{max}}/(E_{\mathrm{max}} + I)}$$

The mean and variance of the truncated distribution are:

$$\begin{aligned}
\langle E_3 \rangle &= \frac{I(E_{\max}+I)}{E_{\max}} \int_I^{E_\alpha} E\, g(E)\, \mathrm{d}E = \frac{I(E_{\max}+I)}{E_{\max}} \ln\left(\frac{E_\alpha}{I}\right) , \\
\langle E_3^2 \rangle &= \frac{I(E_{\max}+I)}{E_{\max}} \int_I^{E_\alpha} E^2\, g(E)\, \mathrm{d}E = \frac{I(E_{\max}+I)}{E_{\max}} (E_\alpha - I) , \\
\sigma_\alpha^2(E_3) &= < E_3^2 > - < E_3 >^2 . \qquad (68)
\end{aligned}$$

Then, the error propagation applied to eq. (66), where N_1, N_2, N_3 and E_3 are random variables, gives:

$$\sigma^2(E) = N_1 e_1^2 + N_2 e_2^2 + N_3 \langle E_3 \rangle^2 + N_3 \sigma_\alpha^2(E_3)(N_3+1) , \qquad (69)$$

where the last two terms come from the variance of a product of two random variables (see Appendix F). For values $\alpha > 0.99$, this variance goes smoothly toward eq. (64) while increasing the absorber thickness.

Now we have to choose for α the values that are useful for our track following. Firstly, we note that the $1/p$ pull spectra obtained with GEANE, in the case of thin absorbers, are composed of a peak, a shoulder near the peak and a very long and flat zone with very few events extending to the left (or the right) of the distribution. The area of the peak plus the shoulder is $> 99\%$ of the total area. We choose α to have a unitary RMS ($\sigma \simeq 1$) for the peak plus the shoulder (see fig. 10).

Using this criterion, after many tracking tests through the PANDA apparatus, we found that a meaningful error propagation, taking into account the core of the distribution and excluding the long δ-electron tail, is obtained with values

$$0.995 \le \alpha \le 0.998 , \qquad (70)$$

In summary, our algorithm calculates the variance of eq. (62) with a variance $\sigma^2(E)$ calculated as follow:

a. for big and moderate absorbers when $\kappa > 0.005$, the variance $\sigma^2(E)$ is given by eq. (61) (old GEANE method);

b. for thin absorbers, $\kappa < 0.005$, when the number of collisions from eq. (65) is $N_c > 50$, $\sigma^2(E)$ is given by eq. (64) with $\alpha = 0.996$ and $\sigma_\alpha = 15.76$;

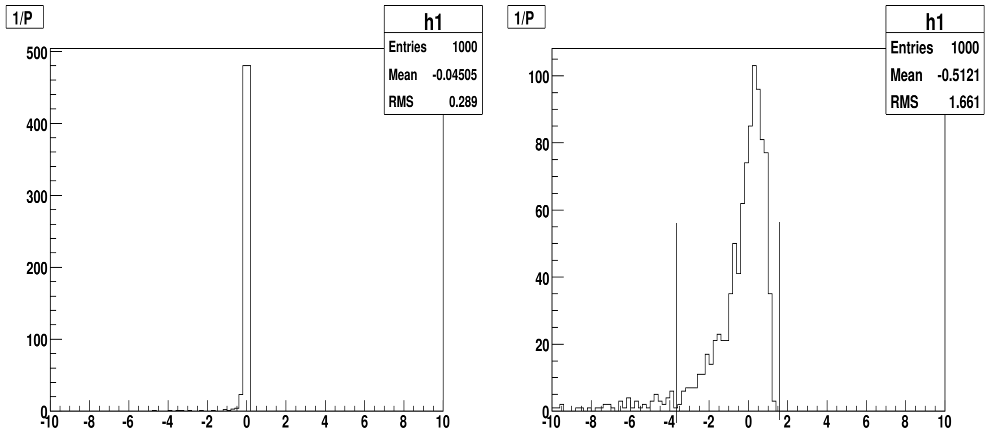

Figure 10: Pull distribution $\Delta(1/p)/\sigma$ for 1 GeV muons after passing through the PANDA straw tube detector. Left: Standard GEANE result (RMS$\simeq 0.3$ in the displayed window); right: result after the modification with $\alpha = 0.995$ (see the text). The region between the vertical lines has RMS$= 1.03$.

c. for very thin absorbers, when $\kappa < 0.005$ and $N_c < 50$, the variance $\sigma^2_\alpha(E)$ is given by eq. (69). The default value for the area considered is $\alpha = 0.996$.

In the new GEANE version, the parameter α is under the control of the user and can be modified (see sect. 9). If one sets $\alpha = 1$ the run uses the old standard GEANE and eq. (61) only is used in the straggling calculation.

Finally, we note that the treatment of the uncertainties due to the energy loss reported here is somewhat arbitrary and based on approximations. Therefore, it has to be tuned, carefully checked and progressively improved by exploiting the experiences of the PANDA users while simulating the apparatus.

The effect of the modifications for PANDA is displayed in fig. 10.

A further improvement could be the inclusion of the fluctuations due to bremsstrahlung for electrons and positrons. This aspect is under study.

8 Use of GEANE in PANDA

The integration of GEANE in pandaroot has been performed at two different levels:

- changes to the class TGeant3 to include all the COMMON data blocks and the functions of the old GEANE;
- changes to the framework with the addition of the new package "geane" with a new C++ interface and some new functionality.

In principle it is possible to call GEANE with the old interface via the VMC class: for this it is sufficient to use a global pointer gMC3 to an object of type TGeant3 and all the historical functions of Geane can be directly used. However in this case input and output handling has to be carefully checked: data structures that map the Fortran COMMON blocks have to be prepared and the output has to be correctly decoded to get meaningful results.

As an alternative a new interface from the pandaroot framework to GEANE is available which simplify the GEANE use and hides the old interface to the user: the new interface is based on a package where the calls to the GEANE code are organized in a set of 5 C++ classes. The classes are the following:

- class **CbmGeane** (inherits from TObject):

  used to initialize GEANE and to read the magnetic field map from the simulation output file;

- class **CbmGeaneHit** (inherits from CbmHit which inherits from TObject):

  used to store the track parameters and their errors before and after the extrapolation into the pandaroot tree (permanent);

- class **CbmGeanePro** (inherits from TNamed):

  used to perform the track extrapolation (here are the calls to the old Fortran routines EUFIL/V/P/L and ERTRAK);

- class **CbmProHit** (inherits from TObject):

  used to store the extrapolation results in memory (transient);

- class **CbmGeaneTr** (inherits from CbmTask which inherits from TTask):

  used to run GEANE as TTask.

The track following is driven by a macro and results are stored in a ROOT tree.

In the new interface we plan to add new functions used to solve some advanced and specific problems. For instance, let consider now the practical case of a user that has found in the MAster Reference System (MARS) the track momentum p by a prefit in a point $\boldsymbol{x} = (x, y, z)$ of the apparatus. To track from x to a detector D he/her has to do, first of all, a transformation from MARS to SC; then there are two options:

1. to work in the SC representation controlling the track length or the tracking volume;

2. to track in the SD representation to the detector planes.

In any case the user will need a routine missing in GEANE that should be present in the interface: to go from MARS to SC. The passage from SC to SD can be done with the other interface routines. We will call this routine From_MARS_To_SC (see tab. 8) and will give here the useful formulas for coding it.

By recalling eqs. (3-5), we can write the SC axes as:

- along the momentum $\boldsymbol{p}$:

$$\begin{aligned} \boldsymbol{x}_\perp &= (\boldsymbol{x}_\perp \cdot \boldsymbol{x})\boldsymbol{x} + (\boldsymbol{x}_\perp \cdot \boldsymbol{y})\boldsymbol{y} + (\boldsymbol{x}_\perp \cdot \boldsymbol{z})\boldsymbol{z} \\ &= (\cos\lambda\cos\phi,\ \cos\lambda\sin\phi,\ \sin\lambda) \end{aligned} \tag{71}$$

- $\boldsymbol{y}_\perp = (\boldsymbol{z} \times \boldsymbol{x}_\perp)/|\boldsymbol{z} \times \boldsymbol{x}_\perp|$ in the $x - y$ plane of MARS and perpendicular to $\boldsymbol{p}$:

$$\begin{aligned} \boldsymbol{y}_\perp &= (\boldsymbol{y}_\perp \cdot \boldsymbol{x})\boldsymbol{x} + (\boldsymbol{y}_\perp \cdot \boldsymbol{y})\boldsymbol{y} + (\boldsymbol{y}_\perp \cdot \boldsymbol{z})\boldsymbol{z} \\ &= (-\sin\phi,\ \cos\phi,\ 0) \end{aligned} \tag{72}$$

  where $\boldsymbol{y}_\perp$ and $\boldsymbol{y}$ are oriented in the same sense;

- $\boldsymbol{x}_\perp \times \boldsymbol{y}_\perp = \boldsymbol{z}_\perp$:

$$\begin{aligned} \boldsymbol{z}_\perp &= (\boldsymbol{z}_\perp \cdot \boldsymbol{x})\boldsymbol{x} + (\boldsymbol{z}_\perp \cdot \boldsymbol{y})\boldsymbol{y} + (\boldsymbol{z}_\perp \cdot \boldsymbol{z})\boldsymbol{z} \\ &= (-\sin\lambda\cos\phi,\ -\sin\lambda\ \sin\phi,\ \cos\lambda) \end{aligned} \tag{73}$$

If the prefit has given the quantities $(1/p, \lambda, \phi)$ and (x, y, z) with their errors (variances and covariances σ_{ij}) in the MARS system, we can find the errors on $y_\perp$ and $z_\perp$. If we suppose no correlation between $(1/p, \lambda, \phi)$ and (x, y, z), from eqs.(71-73) the transport matrix T is given by:

$$T = \left| \begin{array}{ccccc} \frac{\partial 1/p}{\partial 1/p} & \frac{\partial 1/p}{\partial \lambda} & \frac{\partial 1/p}{\partial \phi} & \frac{\partial 1/p}{\partial y} & \frac{\partial 1/p}{\partial z} \\ \frac{\partial \lambda}{\partial 1/p} & \frac{\partial \lambda}{\partial \lambda} & \frac{\partial \lambda}{\partial \phi} & \frac{\partial \lambda}{\partial y} & \frac{\partial \lambda}{\partial z} \\ \frac{\partial \phi}{\partial 1/p} & \frac{\partial \phi}{\partial \lambda} & \frac{\partial \phi}{\partial \phi} & \frac{\partial \phi}{\partial y} & \frac{\partial 1\phi}{\partial z} \\ \frac{\partial y_\perp}{\partial 1/p} & \frac{\partial y_\perp}{\partial \lambda} & \frac{\partial y_\perp}{\partial \phi} & \frac{\partial y_\perp}{\partial y} & \frac{\partial y_\perp}{\partial z} \\ \frac{\partial z_\perp}{\partial 1/p} & \frac{\partial z_\perp}{\partial \lambda} & \frac{\partial z_\perp}{\partial \phi} & \frac{\partial z_\perp}{\partial y} & \frac{\partial z_\perp}{\partial z} \end{array} \right| \tag{74}$$

$$= \left| \begin{array}{ccccc} 1 & 0 & 0 & 0 & 0 \\ 0 & 1 & 0 & 0 & 0 \\ 0 & 0 & 1 & 0 & 0 \\ 0 & 0 & 0 & (\boldsymbol{y}_\perp \cdot \boldsymbol{y}) & (\boldsymbol{y}_\perp \cdot \boldsymbol{z}) \\ 0 & 0 & 0 & (\boldsymbol{z}_\perp \cdot \boldsymbol{y}) & (\boldsymbol{z}_\perp \cdot \boldsymbol{z}) \end{array} \right|$$

where we considered the transformations (72) and (73). The equation (71) on $x_\perp$ is not used because in SC we are on a plane of known coordinate $x_\perp$.

The variances and covariances of $(1/p, \lambda, \phi, y_\perp, z_\perp)$ are given by

$$\sigma_{i,j}^{\mathrm{SC}} = \sum_{kl} T_{ik}\, \sigma_{kl}^{\mathrm{MARS}}\, T_{lj}^{\dagger} \tag{75}$$

Once the input quantities have been prepared bu calling the methods PropagateToPlane(), PropagateToVolume() and PropagateToLength() of the CbmGeanePro class, the tracking can be realized by calling the Propagate() function in the CbmGeanePro class which interfaces the GEANE routine ERTRAK. The input/output sequence of this routine should be:

ERTRAK:
INPUT
X1(3) = starting point (x, y, z) in MARS
P1(3) = starting momentum $1/p, \lambda, \phi$ in MARS
IPA = GEANT particle code
CHOPT =

B = backward tracking

O = tracking without transporting the errors

E = approximated but faster error calculation

L = tracking in SC variables according to the prescribed length defined in EUFILL.

P = tracking in SD variables up to the prescribed planes defined in EUFILP

V = tracking in SC variables to the prescribed volume defined in EUFILV

An example of command could be for example 'BP'. The checks on consistency are made by the routine and trigger a printing (ERTRAK Format 779). A modification could be to transfer an error flag to the interface macro.

OUTPUT

X2(3) = final point (x, y, z) in MARS
P2(3) = final momentum $1/p, \lambda, \phi$ in MARS
IERROR = flag for error conditions (see Format 777, 778 and 779)

The complete output is stored in COMMON blocks and therefore in the Virtual Monte Carlo C++ structs, easily accessible.

The information that have to be taken from the COMMON and passed to the user, step by step, are listed below. They are given *in the system (SC or SD) requested by the tracking routine ERTRAK*:

ERRIN[15] the input covariance matrix in symmetric form;

ERROUT[15] the output covariance matrix in symmetric form;

ERXIN[3] starting coordinates (note that X1 of ERTRAK is in MARS);

ERPIN[3] starting momentum (note that P1 of ERTRAK is in MARS);

ERXOUT[3] output coordinates (note that X2 of ERTRAK is in MARS);

ERPOUT[3] output momentum (note that P2 of ERTRAK is in MARS);

ERTRSP[5,5] transport matrix in single precision;

ERDTSP[5,5] transport matrix in double precision.

Some macros to get this information could also be useful during tracking and Kalman filter coding.

Class	Function	Purpose	Old GEANE correspondence	Notes
CbmPro	From_MARS_To_SC	go from lab system (MARS) to SC system	none	in preparation
CbmPro	From_SC_To_SD	go from SC to SD system	TRSCSD	in preparation
CbmPro	From_SD_To_SC	go from SD to SC system	TRSDSC	in preparation
CbmPro	From_SD1_To_SD2	go from an SD system to another SD system	TRS1S2	in preparation
CbmPro	PropagateToVolume	prepare for tracking	EUFILV	initialization
CbmPro	PropagateToPlane	prepare for tracking	EUFILP	initialization
CbmPro	PropagateToLength	prepare for tracking	EUFILL	preparation
CbmPro	Propagate (V option)	perform a tracking step	ERTRAK	tracking
CbmPro	Propagate (P option)	perform a tracking step	ERTRAK	tracking
CbmPro	Propagate (L option)	perform a tracking step	ERTRAK	tracking
CbmGeaneHit	GetP1,GetLambda1,GetPhi1 GetfY1, GetfZ1	get initial track parameters	none	output
CbmGeaneHit	GetErrorMat	get the initial 15-dim covariance matrix	none	output
CbmGeaneHit	GetP,GetLambda,GetPhi GetfY, GetfZ	get final track parameters	none	output
CbmGeaneHit	GetErrorMat	get the final 15-dim covariance matrix	none	output

Table 2: list of the possible functions for an interface with GEANE

Since the error matrices are symmetric, GEANE uses 15-dim vectors. On the contrary, the transport matrices are 5×5, so that in GEANE some routines perform matrix algebra with symmetric and square matrices. The transformation from a 5×5 symmetric matrix to a triangular 15-dim vector is based on the correspondence

1	2	3	4	5	6	7	8	9	10	11	12	13	14	15
1,1	1,2	1,3	1,4	1,5	2,2	2,3	2,4	2,5	3,3	3,4	3,5	4,4	4,5	5,5

Another important aspect for the user is the correct definition, through the data cards of the modified GEANE version, of two parameters that control the calculation of the energy loss:

GCUT(1): is the parameter α defined in sect. 7, that represents the truncation of the area of the δ-electron energy distribution. It has been introduced by us in the new GEANE version for PANDA. We put as default value $\alpha = 0.995$, but the user can modify it if the pull distribution of the momentum is not satisfactory. If one puts $\alpha = 1$ the energy loss calculation follows the old GEANE method (se sect. 7);

CUTS(8): this is a GEANT parameter of the string CUTS, present also in the old GEANE version. This parameter during the simulation is the upper limit of the energy of the truncated continuos energy loss and the threshold for the δ-ray production. The important difference is that in GEANE, that uses the GEANT routines to find the track mean values, the δ-ray production is not considered; hence, the truncation of the Landau (or straggling) distribution is not followed by the calculation of the energy lost by δ-electron production. This has for the user the following important effects: *if DRAY is small and the Landau distribution is truncated, the average energy is near to the maximium of the distribution; if DRAY is high (i.e. 10 TeV) the tracking follows the full straggling distribution and the tracked value is the average one.*
The choice on what value has to be used depends on the specific case. The standard choice should be the tracking according to the full energy distribution to obtain the mean value. For this reason we put DRAY = 10 TeV as the default value.
Finally, we note that this aspect concern the calculation of the average values only, whereas the error propagation depends on the calculation of the covariance matrix, which is practically independent of this difference on momemntum mean values.

The full GEANE fortran code is available in every standard FairROOT installation in the cbmsoft/transport/geant3 directory. Moreover the complete cards of GEANE 3.21 can be downloaded for example by:

http://xrootd.slac.stanford.edu/BFROOT/src/geant/94b/geane321.car

9 Some results with the PANDA geometry

We checked the GEANE performances with a set of simulated data with the PANDA geometry. The multiple scattering has been simulated with the Molière distribution.

The pull or standard variables

$$T = \frac{(x_{\mathrm{GEANE}} - X_{sim})}{\sigma_{\mathrm{GEANE}}} \; , \qquad x = [1/p, \lambda, \phi, y, z]$$

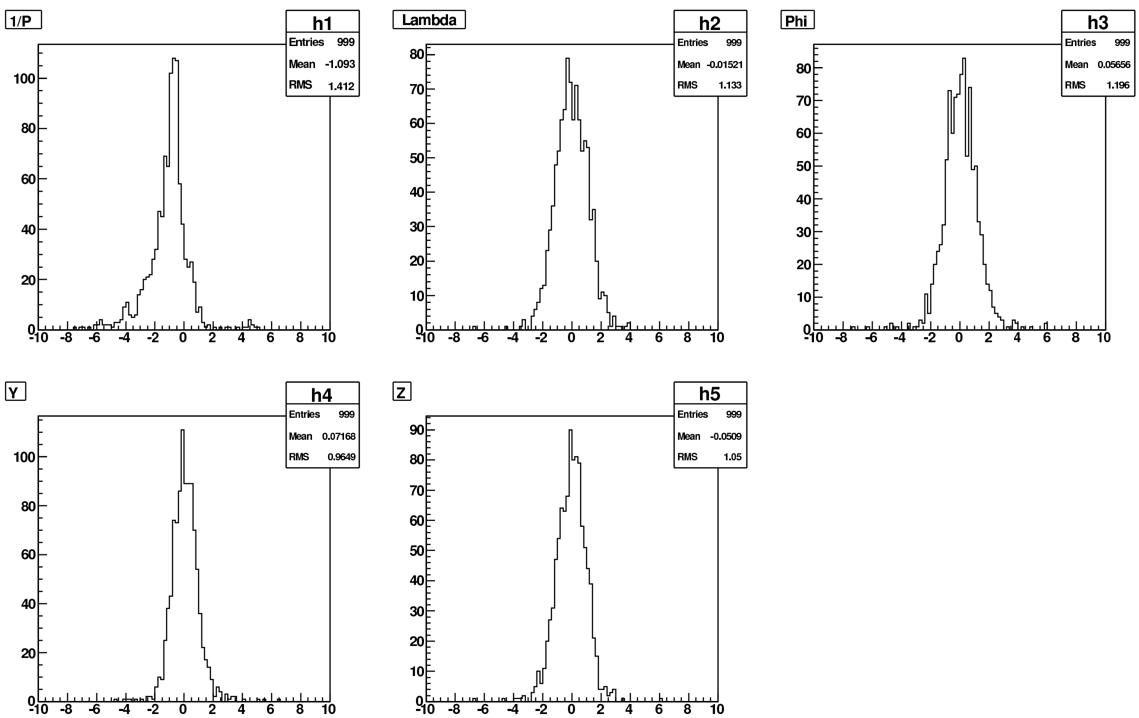

Figure 11: Pull distributions of the 5 track parameters in the case of 2 GeV muons that have passed through the whole detector, just before the PANDA magnet.

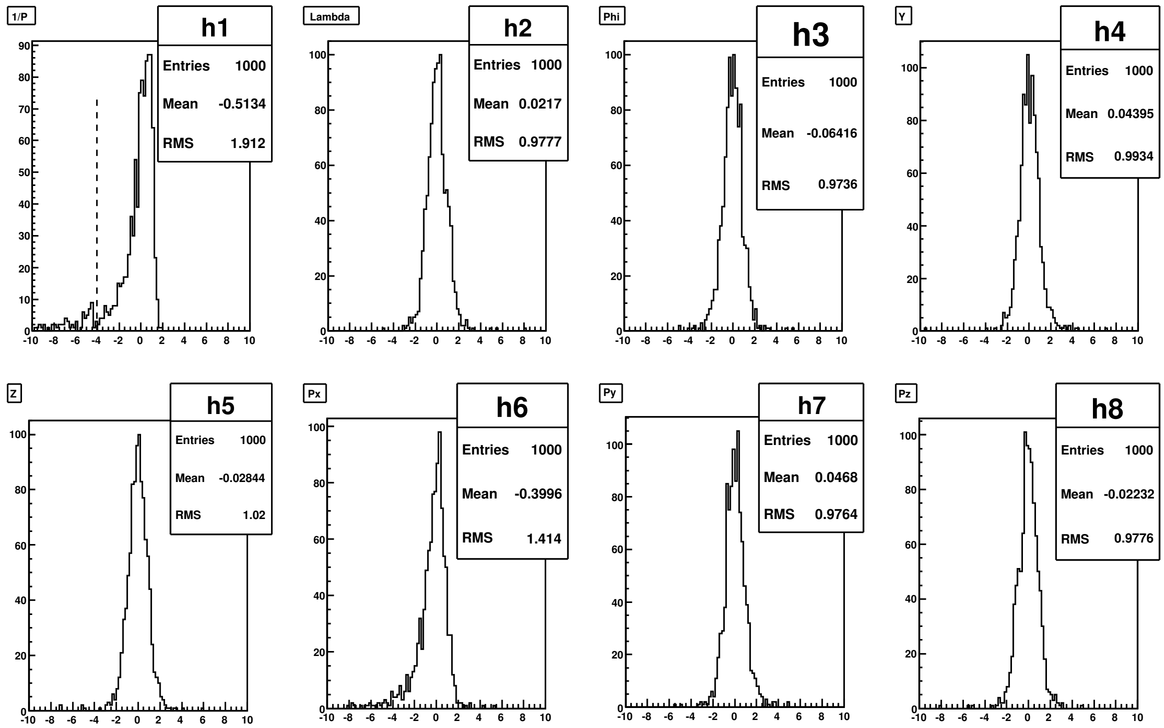

Figure 12: Pull distributions of the 5 track parameters and of p_x, p_y, p_z in the case of 2 GeV muons after passing through the 22 layers of the straw tube detector only. For the $1/p$ histogram dispersion up to the dotted line one has RMS$= 1.08$ (top left).

for the 5 track parameters are shown in the case of 2 GeV muons in a plane immediately before the magnet are shown in fig. 11, wheras the same quantities after the straw tube detector are shown in fig. 12. The shape of the distributions, apart from that of $1/p$, is near to the standard gaussian with $\sigma[T] \simeq 1$, as expected.

The root mean square (RMS) of the coordinates y and z is $\simeq 1$ for the raw simulated data, whereas the fitted gaussian has $\sigma \simeq 0.9$. This is an expected effect due to the non gaussian tails of the Molière multiple scattering distribution.

The agreement between the track following and the simulation is good. Results of similar quality are obtained between 0.5 and 10 GeV, with detection planes put in different positions of the PANDA apparatus.

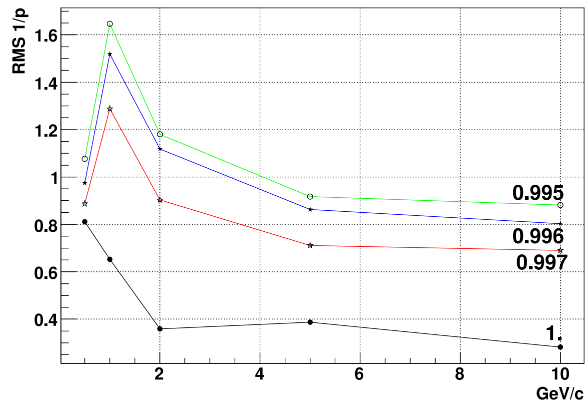

Figure 13: Behaviour of the σ of the $1/p$ pull distributions with energy, parametrized with the truncation parameter α of tab.1.

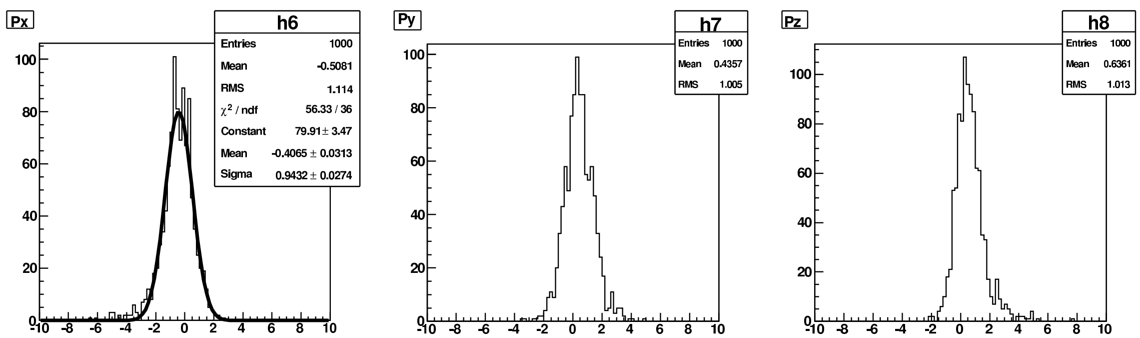

Figure 14: Pull quantities for the momentum components p_x, p_y, p_z for 5 GeV pions after the whole detector immediately before the PANDA magnet.

The uncertainty in the error calculation for $1/p$ has been explored as a function of the truncation parameter α of tab. 1. The suggested value for PANDA is $\alpha = 0.996$. The value $\alpha = 1$ uses the original GEANE calculation (see sect.7).

In figs. 12 and 14 the pulls of the momentum components for muons and pions are shown. These plots are important to test the correctness of the $1/p$ error propagation and of some non diagonal elements of the GEANE covariance matrix. For example, $p_x = p \cos\lambda \cos\phi$ and

$$\frac{\partial p_x}{\partial p} = \cos\lambda\cos\phi \ , \quad \frac{\partial p_x}{\partial \lambda} = -p\sin\lambda\cos\phi \ , \quad \frac{\partial p_x}{\partial \phi} = -p\cos\lambda\sin\phi \ ,$$

the variance is given by

$$\sigma^2[p_x] = \sum_{ij} \frac{\partial p_x}{\partial x_i}\, \sigma[x_i, x_j] \ , \quad \sigma[x_i, x_i] \equiv \sigma^2_{x_i} \ , \tag{76}$$

where $x_i = [p, \lambda, \phi]$ and the non diagonal elements of the tracking covariance matrix involved in the calculations are $\sigma[1/p, \lambda]$, $\sigma[1/p, \phi]$, $\sigma[\lambda, \phi]$:

$$\sigma^2_p = p^4 \sigma^2_{1/p} \ , \quad \sigma[p, \lambda] = -p^2 \sigma[1/p, \lambda] \ , \quad \sigma[p, \phi] = -p^2 \sigma[1/p, \phi] \ .$$

10 Application to Kalman filter

One of the best ways to understand the filter algorithms, as the Kalman one, is to start from the χ^2 minimization

$$\chi^2(\mu) = \frac{(x_1 - \mu)^2}{\sigma_1^2} + \frac{(x_2 - \mu)^2}{\sigma_2^2} \tag{77}$$

obtaining, with the equation $\partial \chi^2(\mu)/\partial \mu = 0$, the well know estimation of μ through the average of the two measured values x_1 and x_2 weighted on the two errors σ_1 and σ_2:

$$\mu = \frac{x_1/\sigma_1^2 + x_2/\sigma_2^2}{1/\sigma_1^2 + 1/\sigma_1^2} \ , \qquad \mathrm{Var}[\mu] = \frac{1}{1/\sigma_1^2 + 1/\sigma_2^2} = \frac{\sigma_1^2\, \sigma_2^2}{\sigma_1^2 + \sigma_2^2} \ . \tag{78}$$

The estimator (78), in the case of gaussian variables, exploits the properties of both the Least Squares (LS) and Maximum Likelihood (ML) estimators [1]. This is elementary statistics.

After a simple algebraic manipulation, one can write eq. (78) in the so-called recursive form:

$$\mu \ = \ x_1 + \frac{\sigma_1^2}{\sigma_1^2 + \sigma_2^2}(x_2 - x_1) \equiv x_1 + K(x_2 - x_1) \tag{79}$$

$$\mathrm{Var}[\mu] \ = \ \sigma_1^2 - K\sigma_1^2 = (1 - K)\, \sigma_1^2 \ , \tag{80}$$

where the term multiplied by the *gain factor* K appears as a correction to the initial value x_1 in eq. (79) and as a reduction of the initial uncertainty σ_1 in eq. (80).

Now we consider the track points of Fig. (15) and try to find the best estimation of the true track point f_i at the i-th detector plane by minimizing the $\chi 2$ (see Tab. 3 for the meaning of the symbols):

$$\chi^2(\boldsymbol{f}) = \sum_i [(\boldsymbol{e}_i[\boldsymbol{f}_{i-1}]-\boldsymbol{f}_i)\boldsymbol{W}_{i-1,i}(\boldsymbol{e}_i[\boldsymbol{f}_{i-1}]-\boldsymbol{f}_i)]+(\boldsymbol{x}_i-\boldsymbol{f}_i)\boldsymbol{V}_i(\boldsymbol{x}_i-\boldsymbol{f}_i) \quad (81)$$

In this equation we emphasize that the extrapolation $\boldsymbol{e}$ starts from the true points $\boldsymbol{f}_i$ and that for this reason to these points is associated the weight matrix $\boldsymbol{W}$ containing the tracking errors only. Remember also that the bold face symbols recall that we are dealing with 5-fold vectors considered at the i-th detector plane and with 5×5 matrices (written in capital letters).

The minimization of eq. (81) gives:

$$\begin{aligned} \frac{\partial \chi^2}{\partial \boldsymbol{f}_i} &= \boldsymbol{W}_{i-1,i}(\boldsymbol{e}_i[\boldsymbol{f}_{i-1}]-\boldsymbol{f}_i)+\boldsymbol{V}(\boldsymbol{x}_i-\boldsymbol{f}_i) \\ &\quad -\boldsymbol{T}(l_{i+1},l_i)\,\boldsymbol{W}_{i,i+1}(\boldsymbol{e}_{i+1}[\boldsymbol{f}_i]-\boldsymbol{f}_{i+1}) = 0\ , \end{aligned} \quad (82)$$

where eq. (12) has been used. The first two terms appear usually in χ^2 minimizations (producing the weighted average estimator between the ex-

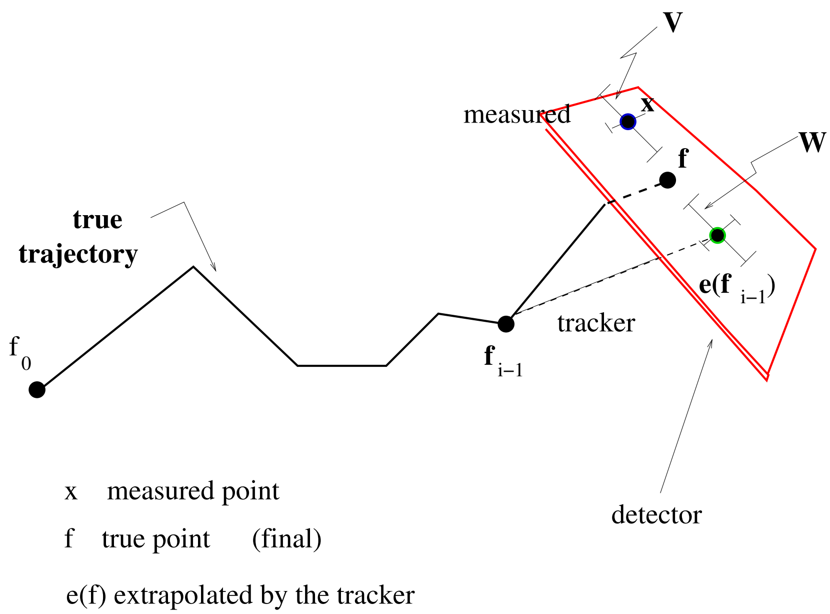

Figure 15: Definition of terms in eq. (81).

trapolation $\boldsymbol{e}$ and the i-th measurement $\boldsymbol{x}$), whereas here appears an extra third term, due to the f-dependence of the track follower operator $\boldsymbol{G}(l_j) = \boldsymbol{e}_j(\boldsymbol{f}_{j-1})$.

The Kalman filter *is precisely a method to solve eq.* (82). It was originally proposed in 1961 by the MIT engineer Kalman in the framework of the control and optimization theory of systems [7] and applied successively in particle physics as a useful track fitting technique [8].

The resolution of eq. (82) is cumbersome. A rather clear demonstration can be found in [5]. Here we report the solution in the form of the so-called three-steps Kalman filter algorithm [5, 1]. In what follows the notation $\sigma^2[\cdot]$ will be used for the covariance matrix of a track vector.

The first step is the *extrapolation* with eqs. (10, 14) of the previous Kalman value $\boldsymbol{k}_{i-1}$ to the i-th plane:

$$\boldsymbol{e}_i \equiv \boldsymbol{e}_i(\boldsymbol{k}_{i-1}) = \boldsymbol{G}(\boldsymbol{k}_{i-1}) \tag{83}$$

$$\boldsymbol{\sigma}^2[\boldsymbol{e}_i] = \boldsymbol{T}(l_i, l_{i-1})\, \boldsymbol{\sigma}^2[\boldsymbol{k}_{i-1}]\, \boldsymbol{T}^T(l_i, l_{i-1}) + \boldsymbol{W}^{-1}_{i-1,i} \tag{84}$$

The second step is the calculation of the *Kalman filter value* at the i-th detector plane:

$$\boldsymbol{k}_i = \boldsymbol{\sigma}^2[\boldsymbol{k}_i] \left(\boldsymbol{\sigma}^{-2}[\boldsymbol{e}_i]\, \boldsymbol{e}_i + \boldsymbol{V}_i \boldsymbol{x}_i\right) \tag{85}$$

$$\boldsymbol{\sigma}^{-2}[\boldsymbol{k}_i] = \boldsymbol{\sigma}^{-2}[\boldsymbol{e}_i] + \boldsymbol{V}_i \tag{86}$$

These equations are simply the weighted average (78) in the 5-fold track space.

The third step is the *backward smoothing* of the Kalman point solution of the second step:

$$\boldsymbol{f}_i = \boldsymbol{k}_i + \boldsymbol{A}_i\,(\boldsymbol{f}_{i+1} - \boldsymbol{e}_{i+1}) \tag{87}$$

$$\boldsymbol{\sigma}^2[\boldsymbol{f}_i] = \boldsymbol{\sigma}^2[\boldsymbol{k}_i] + \boldsymbol{A}_i \left(\boldsymbol{\sigma}^2[f_{i+1}] - \boldsymbol{\sigma}^2[\boldsymbol{e}_{i+1}]\right) \boldsymbol{A}_i^T \tag{88}$$

$$\boldsymbol{A}_i = \boldsymbol{\sigma}^2[\boldsymbol{k}_i]\, \boldsymbol{T}^T(l_{i+1}, l_i)\, \boldsymbol{\sigma}^{-2}[\boldsymbol{e}_{i+1}] \tag{89}$$

After these three steps one obtains as a solution the track points $\boldsymbol{f}_i$ and their uncertainties at the i-th plane. These values are the solution of eq. (82), that is the best estimate, in the LS sense, of the true track.

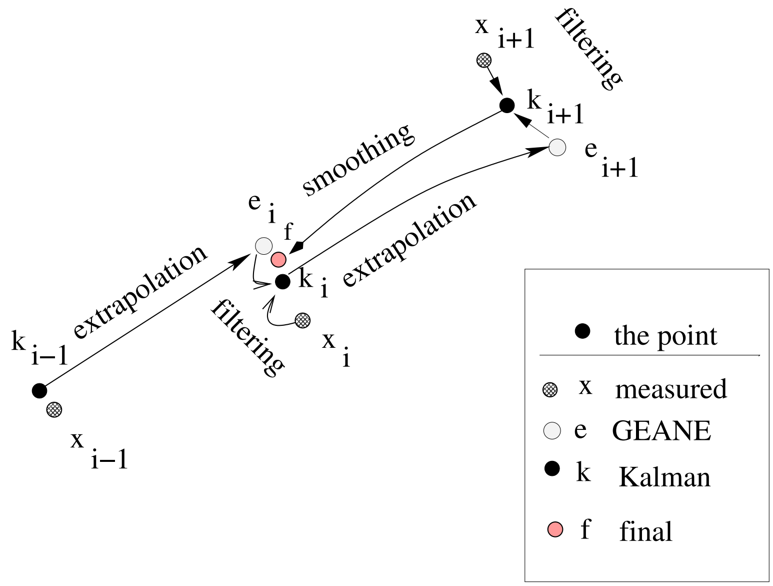

Figure 16: Extrapolation (GEANE), Kalman filtering and smoothing at the i-th detector plane (see the text for details).

The scheme of eqs. (83-89) is sketched in Fig 16.

The second step, the Kalman filtering, can be also expressed in the *gain K-matrix* form, similar to eqs. (79, 80) [8]:

$$\boldsymbol{k}_i = \boldsymbol{e}_i + \boldsymbol{K}_i(\boldsymbol{x}_i - \boldsymbol{e}_i) \tag{90}$$

$$\boldsymbol{\sigma}^2[\boldsymbol{k}_i] = (\boldsymbol{I} - \boldsymbol{K})\, \boldsymbol{\sigma}^2[\boldsymbol{e}_i] \tag{91}$$

$$\boldsymbol{K}_i = \boldsymbol{\sigma}^2[\boldsymbol{e}_i]\,(\boldsymbol{V}^{-1} + \boldsymbol{\sigma}^2[\boldsymbol{e}_i])^{-1}\ . \tag{92}$$

Up to this point we supposed that the track follower and all the measured points are expressed with the same set of track variables. To take into account that this could not be the case, sometime a matrix $\boldsymbol{H}$ is introduced, which makes comparable the two representations:

$$\boldsymbol{x}_i = \boldsymbol{H}_i\boldsymbol{e}_i + \epsilon_i\ , \tag{93}$$

where ϵ is the random part introduced by the measurement. The expression of the filter with the $\boldsymbol{H}$ matrix explicitly written can be found in [1, 8].

11 Conclusions

The first aim of this report is to collect and write explicitly all the useful formulae for the error propagation in track following. The basic element is the transport matrix of eq. (12):

$$T_{ij}(l_2, l_1) = \frac{\partial e^i(l_2)}{\partial e^j(l_1)} \ ,$$

where $\boldsymbol{e}(l)$ is the extrapolated trajectory with track length l with error $\delta\boldsymbol{e}(l)$:

$$\delta\boldsymbol{e}(l_2) = \boldsymbol{T}(l_2, l_1)\, \delta\boldsymbol{e}(l_1) \ .$$

The error propagation is then obtained with the fundamental formula (14) that we rewrite here:

$$\boldsymbol{\sigma}^2(l_2) = \boldsymbol{T}(l_2, l_1)\, \boldsymbol{\sigma}^2(l_1)\, \boldsymbol{T}^T(l_2, l_1) + \boldsymbol{W}^{-1}(l_1) \ , \tag{94}$$

In this scheme the calculation of the transport matrix is made by repeated applications of an infinitesmal (numerically small) transformation ($\mathrm{d}l = (l_2 - l_1)/n$):

$$\boldsymbol{T}(l_2, l_1) = \lim_{dl \to 0} (\prod_{j=1}^{n} \boldsymbol{F}_j) \ .$$

Then, the track following problem consists, first of all, in finding the matricial form of the infinitesimal operator F, that in GEANE is written in term of two matrices $\boldsymbol{A}$ (without magnetic effects) and $\boldsymbol{B}$ (that contains the magnetic effects):

$$\boldsymbol{F}_l = \boldsymbol{I} + (\boldsymbol{A}_{l+dl} + \boldsymbol{B}_{l+dl}) \cdot \mathrm{d}l \ ,$$

The explicit form of the matrices A and B has been given in eqs. (31) and (42). This solves the first term of eq. (94), which propagates the errors step by step.

At each step, the multiple scattering and energy loss effects are supposed incorrelated and are added in the matrix $\boldsymbol{W}^{-1}$. The explicit form of the multiple scattering error matrix has been given in eq. (57), where the value of the GEANE r.m.s. multiple scattering angle has been corrected using an expression taken from [10].

Then, the energy loss fluctuactions, that have to be put in the place W_{11}^{-1}, have been considered. It is important to note that this point has not a rigorous solution in track following, because the fluctuactions in very thin absorbers give a variance $\sigma^2(E)$ very large or undefined. We tried to insert in the GEANE structure some recent developments from the Urban model, see eq. (69). Since probably at present this aspect is not fully under control, the results have to be checked carefully for the PANDA detectors and energies. The interface with GEANE has been modified to be flexible enough to allow tests and comparisons between the various approaches.

The first tests wih this new GEANE interface have been shown, with results good enough to allow the application of this track following to the global fits.

In this context, we have shown how we are implementing the Kalman filter global fit by using the GEANE track following. The results will be shown in a forthcoming report.

12 Appendices

Appendix A
Infinitesimal rotation matrix between two transverse reference systems.

Without loss of generality, we can evaluate the transformation in $\phi = 0$. Equation (9), which reads

$$\begin{pmatrix} x_\perp \\ y_\perp \\ z_\perp \end{pmatrix} = \begin{pmatrix} \cos\lambda\cos\phi & \cos\lambda\sin\phi & \sin\lambda \\ -\sin\phi & \cos\phi & 0 \\ -\sin\lambda\cos\phi & -\sin\lambda\sin\phi & \cos\lambda \end{pmatrix} \begin{pmatrix} x \\ y \\ z \end{pmatrix} , \quad (95)$$

becomes, to the first order in $\phi = 0$:

$$\begin{aligned} \begin{pmatrix} x'_\perp \\ y'_\perp \\ z'_\perp \end{pmatrix} &= \begin{pmatrix} \cos\lambda - \mathrm{d}\lambda\sin\lambda & \cos\lambda\,\mathrm{d}\phi & \sin\lambda + \mathrm{d}\lambda\cos\lambda \\ \mathrm{d}\phi & 1 & 0 \\ -\sin\lambda - \mathrm{d}\lambda\cos\lambda & -\mathrm{d}\phi\sin\lambda & \cos\lambda - \mathrm{d}\lambda\sin\lambda \end{pmatrix} \begin{pmatrix} x \\ y \\ z \end{pmatrix} \\ &= \begin{pmatrix} \cos\lambda & 0 & \sin\lambda \\ 0 & 1 & 0 \\ -\sin\lambda & 0 & \cos\lambda \end{pmatrix} \begin{pmatrix} x \\ y \\ z \end{pmatrix} + \mathrm{d}\lambda \begin{pmatrix} -\sin\lambda & 0 & \cos\lambda \\ 0 & 0 & 0 \\ -\cos\lambda & 0 & -\sin\lambda \end{pmatrix} \begin{pmatrix} x \\ y \\ z \end{pmatrix} + \\ &+ \mathrm{d}\phi \begin{pmatrix} 0 & \cos\lambda & 0 \\ -1 & 0 & 0 \\ 0 & -\sin\lambda & 0 \end{pmatrix} \begin{pmatrix} x \\ y \\ z \end{pmatrix} \end{aligned} \quad (96)$$

Inverting (95), i.e. making the transpose for $\phi = 0$:

$$\begin{pmatrix} x \\ y \\ z \end{pmatrix} = \begin{pmatrix} \cos\lambda & 0 & -\sin\lambda \\ 0 & 1 & 0 \\ \sin\lambda & 0 & \cos\lambda \end{pmatrix} \begin{pmatrix} x_\perp \\ y_\perp \\ z_\perp \end{pmatrix} \quad (97)$$

and inserting it in (96) we get

$$\begin{aligned} \begin{pmatrix} x'_\perp \\ y'_\perp \\ z'_\perp \end{pmatrix} &= \begin{pmatrix} 1 & 0 & 0 \\ 0 & 1 & 0 \\ 0 & 0 & 1 \end{pmatrix} \begin{pmatrix} x_\perp \\ y_\perp \\ z_\perp \end{pmatrix} + \mathrm{d}\lambda \begin{pmatrix} 0 & 0 & 1 \\ 0 & 0 & 0 \\ -1 & 0 & 0 \end{pmatrix} \begin{pmatrix} x_\perp \\ y_\perp \\ z_\perp \end{pmatrix} + \\ &+ \mathrm{d}\phi \begin{pmatrix} 0 & \cos\lambda & 0 \\ -\cos\lambda & 0 & \sin\lambda \\ 0 & -\sin\lambda & 0 \end{pmatrix} \begin{pmatrix} x_\perp \\ y_\perp \\ z_\perp \end{pmatrix} \end{aligned} \quad (98)$$

$$= \begin{pmatrix} 1 & \mathrm{d}\phi\cos\lambda & \mathrm{d}\lambda \\ -\mathrm{d}\phi\cos\lambda & 1 & \mathrm{d}\phi\sin\lambda \\ -\mathrm{d}\lambda & -\mathrm{d}\phi\sin\lambda & 1 \end{pmatrix} \begin{pmatrix} x_\perp \\ y_\perp \\ z_\perp \end{pmatrix} \quad (99)$$

$$= \begin{pmatrix} 1 & d\gamma & -d\beta \\ -d\gamma & 1 & \tan\lambda d\gamma \\ d\beta & -\tan\lambda d\gamma & 1 \end{pmatrix} \begin{pmatrix} x_\perp \\ y_\perp \\ z_\perp \end{pmatrix} \quad (100)$$

where the last passage comes putting $\mathrm{d}\lambda = -d\beta$ and $\mathrm{d}\phi\cos\lambda = d\gamma$.

Appendix B
Calculations for eq.(22)

Let' s divide, as described in the text, the length L of the track into n small steps $dl = \frac{L}{n}$ and let' s apply equation (22) for each step

$$\begin{aligned} (\delta\vec{x})_L &= F_L(\delta\vec{x})_{L-dl} + (\delta\vec{x}^M)_L \\ (\delta\vec{x})_{L-dl} &= F_{L-dl}(\delta\vec{x})_{L-2dl} + (\delta\vec{x}^M)_{L-dl} \\ (\delta\vec{x})_{L-2dl} &= F_{L-2dl}(\delta\vec{x})_{L-3dl} + (\delta\vec{x}^M)_{L-2dl} \\ &\dots \\ (\delta\vec{x})_{L-(n-1)dl} &= F_{L-(n-1)dl}(\delta\vec{x})_0 + (\delta\vec{x}^M)_{L-(n-1)dl} \\ & (L-(n-1)dl = dl) \end{aligned}$$

In general $(\delta\vec{x})_{ndl}$ can be written

$$\begin{aligned} (\delta\vec{x})_{ndl} &= F_L[F_{L-dl}(\delta\vec{x})_{L-2dl} + (\delta\vec{x}^M)_{L-dl}] + (\delta\vec{x}^M)_L \\ &= F_L F_{L-dl}(\delta\vec{x})_{L-2dl} + F_L(\delta\vec{x}^M)_{L-dl} + (\delta\vec{x}^M)_L \\ &= F_L F_{L-dl}[F_{L-2dl}(\delta\vec{x})_{L-3dl} + (\delta\vec{x}^M)_{L-2dl}] + F_L(\delta\vec{x}^M)_{L-dl} + (\delta\vec{x}^M)_L \\ &= F_L F_{L-dl} F_{L-2dl}(\delta\vec{x})_{L-3dl} + F_L F_{L-dl}(\delta\vec{x}^M)_{L-2dl} + \\ &\quad + F_L(\delta\vec{x}^M)_{L-dl} + (\delta\vec{x}^M)_L \\ &= \dots \end{aligned}$$

that can be rewritten (putting L= ndl, and writing $F_L = F_n$ and so on)

$$(\delta\vec{x})_L = F_n F_{n-1} F_{n-2} \dots F_1 (\delta\vec{x})_0 + (a)$$

$$\left.\begin{array}{lll} + & F_nF_{n-1}...F_2(\delta\vec{x}^M)_1 & + \\ + & F_nF_{n-1}...F_3(\delta\vec{x}^M)_2 & + \\ + & ... & + \\ + & F_nF_{n-1}(\delta\vec{x}^M)_{n-2} & + \\ + & F_n(\delta\vec{x}^M)_{n-1} & + \end{array}\right\} (b)$$

$$+ \quad (\delta\vec{x}^M)_n \qquad (c)$$

Part (a) can be written:

$$(\prod_{i=0}^{n-1} F_{n-i})(\delta\vec{x})_0 = \prod_{j=n}^{1} F_j(\delta\vec{x})_0 \ , \qquad (101)$$

whereas part(b) becomes:

$$\sum_{v=1}^{n-1}[\prod_{j=n}^{v+1} F_j(\delta\vec{x}^M)_v] \ , \qquad (102)$$

obtaining equation (22).

Appendix C
Calculation of the $\frac{1}{p}$ error.

With reference to the figure, we have:

$$\left\{\begin{array}{l} \frac{\delta\left(\frac{1}{p}\right)_{l+dl}}{\delta(\mathrm{d}l)} = \left(\frac{d\frac{1}{p}}{dl}\right)_{l+dl} \\ \frac{\delta\left(\frac{1}{p}\right)_{l}}{\delta(\mathrm{d}l)} = \left(\frac{d\frac{1}{p}}{dl}\right)_{l} \end{array}\right.$$

$$\frac{\delta\left(\frac{1}{p}\right)_{l+dl}}{\delta\left(\frac{1}{p}\right)_{l}} = \frac{\left(\frac{d\frac{1}{p}}{dl}\right)_{l+dl}}{\left(\frac{d\frac{1}{p}}{dl}\right)_{l}}$$

Demonstration of the second part of equation (30)

$$f(x) \ = \ f(x_0) + f'(x_0)(x - x_0)$$

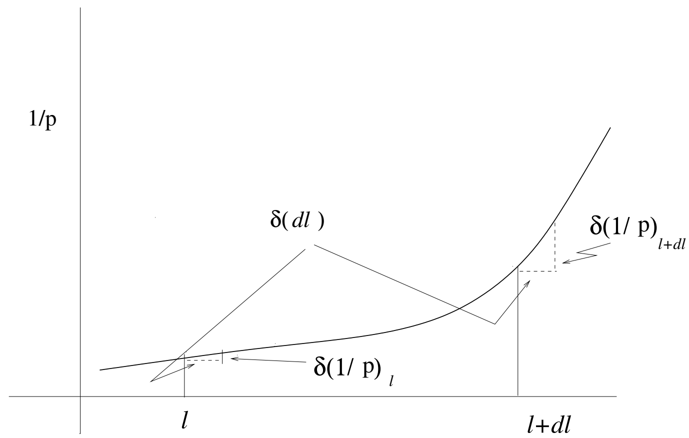

Figure 17: Error propagation on $1/p$ as a function of the traversed thickness. The error $\delta(\,\mathrm{d}l)$ is considered constant. The error on $1/p$ is different when moving from l to $(l+dl)$ as shown in this figure and depends on the range-momentum relationship.

$$\left(\frac{d\frac{1}{p}}{dl}\right)_{l+dl} = \left(\frac{d\frac{1}{p}}{dl}\right)_l + \frac{d}{dl}\left(\frac{d\frac{1}{p}}{dl}\right)_l dl$$

$$\frac{\left(\frac{d\frac{1}{p}}{dl}\right)_{l+dl}}{\left(\frac{d\frac{1}{p}}{dl}\right)_l} = \frac{\left(\frac{d\frac{1}{p}}{dl}\right)_l + \left(\frac{d^2\frac{1}{p}}{dl^2}\right)_l dl}{\left(\frac{d\frac{1}{p}}{dl}\right)_l}$$

$$= \left[1 + \frac{\left(\frac{d^2\frac{1}{p}}{dl^2}\right)}{\left(\frac{d\frac{1}{p}}{dl}\right)} \cdot dl\right]$$

Appendix D
Transformation of the magnetic field H

From equation (9)

$$\begin{pmatrix} H_1 \\ H_2 \\ H_3 \end{pmatrix} = \begin{pmatrix} \cos\lambda\cos\phi & \cos\lambda\sin\phi & \sin\lambda \\ -\sin\phi & \cos\phi & 0 \\ -\sin\lambda\cos\phi & -\sin\lambda\sin\phi & \cos\lambda \end{pmatrix} \begin{pmatrix} H_x \\ H_y \\ H_z \end{pmatrix}$$

$$\begin{cases} H_1 &= H_x \cos\lambda \cos\phi + H_y \cos\lambda \sin\phi + H_z \sin\lambda \\ H_2 &= -H_x \sin\phi + H_y \cos\phi \\ H_3 &= -H_x \sin\lambda \cos\phi - H_y \sin\lambda \sin\phi + H_z \cos\lambda \end{cases}$$

$$\begin{cases} H_1 &= \cos\lambda(H_x \cos\phi + H_y \sin\phi) + H_z \sin\lambda = \\ &= H_0 \cos\lambda + H_z \sin\lambda \\ H_2 &= -H_x \sin\phi + H_y \cos\phi \\ H_3 &= -\sin\lambda(H_x \cos\phi + H_y \sin\phi) + H_z \cos\lambda = \\ &= -H_0 \sin\lambda + H_z \cos\lambda \end{cases}$$

$$\begin{cases} H_0 &= H_x \cos\phi + H_y \sin\phi = -\frac{dH_2}{d\phi} = -(-H_x \cos\phi - H_y \sin\phi) \\ H_1 &= H_0 \cos\lambda + H_z \sin\lambda = -\frac{dH_3}{d\lambda} = -(-H_0 \cos\lambda - H_z \sin\lambda) \\ H_2 &= -H_x \sin\phi + H_y \cos\phi = \frac{dH_0}{d\phi} = (-H_x \sin\phi + H_y \cos\phi) \\ H_3 &= -H_0 \sin\lambda + H_z \cos\lambda = \frac{dH_1}{d\lambda} = (-H_0 \sin\lambda + H_z \cos\lambda) \end{cases}$$

Appendix E
Magnetic field derivatives

Here we calculates the variation:

$$\delta \begin{pmatrix} -H_2 \\ \frac{H_3}{\cos\lambda} \end{pmatrix}$$

. For $\delta(-H_2)$:

$$\begin{aligned} \delta(-H_2) &= -\frac{\mathrm{d}H_2}{\mathrm{d}\lambda}\delta\lambda - \frac{\mathrm{d}H_2}{\mathrm{d}\phi}\delta\phi \\ &= \underbrace{(+\frac{\mathrm{d}H_x}{\mathrm{d}\lambda}\sin\phi - \frac{\mathrm{d}H_y}{\mathrm{d}\lambda}\cos\phi)}_{0}\,\delta\lambda + H_0\,\delta\phi \end{aligned}$$

For $\delta(\frac{H_3}{\cos\lambda})$:

$$\delta(\frac{H_3}{\cos\lambda}) = \frac{\mathrm{d}}{\mathrm{d}\lambda}(\frac{H_3}{\cos\lambda})\delta\lambda - \frac{\mathrm{d}}{\mathrm{d}\phi}(\frac{H_3}{\cos\lambda})\delta\phi$$

$$
\begin{aligned}
&= \frac{\frac{\mathrm{d}H_3}{\mathrm{d}\lambda}\cos\lambda + H_3\sin\lambda}{\cos^2\lambda}\delta\lambda + \frac{\frac{\mathrm{d}H_3}{\mathrm{d}\phi}}{\cos\lambda}\delta\phi \\
&= \frac{-H_1 + H_3\tan\lambda}{\cos\lambda}\,\delta\lambda - \frac{H_2\sin\lambda}{\cos\lambda}\delta\phi \\
&= -\frac{H_1}{\cos^2\lambda}\,\delta\lambda - H_2\tan\lambda\,\delta\phi
\end{aligned}
$$

In conclusion

$$
\delta\begin{pmatrix} -H_2 \\ \frac{H_3}{\cos\lambda} \end{pmatrix} = \begin{pmatrix} 0 \\ \frac{-H_1+H_3\tan\lambda}{\cos\lambda} \end{pmatrix}\delta\lambda + \begin{pmatrix} H_0 \\ -H_2\tan\lambda \end{pmatrix}\delta\phi
$$

Appendix F
Variance of the product of independent variables

If X and Y are two independent random variables having density distribution $p_X(x)$ and $p_Y(y)$ respectively, the variance of their product is given by:

$$
\begin{aligned}
\mathrm{Var}[XY] &= \int (xy - <x><y>)^2 p_X(x)p_Y(y)\,\mathrm{d}x\,\mathrm{d}y \\
&= \int x^2y^2 + <x>^2<y>^2 - 2<x><y>x\,y\,p_X(x)p_Y(y)\,\mathrm{d}x\,\mathrm{d}y \\
&= <x^2><y^2> + <x>^2<y>^2 - 2<x>^2<y>^2 \\
&= <x^2><y^2> - <x>^2<y>^2 \\
&= (\sigma_x^2 + <x>^2)(\sigma_y^2 + <y>^2) - <x>^2<y>^2 \\
&= \sigma_x^2\sigma_y^2 + \sigma_y^2 <x>^2 + \sigma_x^2 <y>^2 \quad .
\end{aligned}
$$

The relative error is given by:

$$
\frac{\mathrm{Var}[XY]}{<x>^2<y>^2} = \frac{\sigma_x^2}{<x>^2} + \frac{\sigma_y^2}{<y>^2} + \frac{\sigma_x^2\sigma_y^2}{<x>^2<y>^2}
$$

and the usual rule of the addition of the relative errors is rediscovred at the first order when the relative variances are small

Appendix G
Symbols used in the report

symbol	meaning
l	track length
$\boldsymbol{X} = X^a$, $(a = 1, 2 \ldots 5)$	random values of track parameters
$\boldsymbol{f}_i = f_i^a$, $(a = 1, 2 \ldots 5)$	true track parameters (mean values) at detector plane i
$\boldsymbol{x}_i = x_i^a$, $(a = 1, 2 \ldots 5)$	measured track parameters at detector plane i
$\boldsymbol{k}_i = k_i^a$, $(a = 1, 2 \ldots 5)$	Kalman-filtered track parameters at detector plane i
$\boldsymbol{e}_i = e_i^a(l)$, $(a = 1, 2 \ldots 5)$	extrapolated track parameters at detector plane i
$\boldsymbol{C}^2$	measurement covariance matrix
$C_{ij}^2 \quad (i, j = 1, 2 \ldots 5)$	elements of C^2
$\boldsymbol{V} = (\boldsymbol{C}^2)^{-1}$	measurement weight matrix
$V_{ij} \quad (i, j = 1, 2 \ldots 5)$	elements of V
$\boldsymbol{\sigma}^2[\cdot]$	track following (tracker) covariance matrix
σ_{ij}^2	elements of σ^2
$\boldsymbol{W} = (\boldsymbol{\sigma}^2)^{-1}$	tracker weight matrix
$W_{ij} \quad (i, j = 1, 2 \ldots 5)$	elements of W
$\boldsymbol{G}(\cdot)$	operator (GEANE) for track following
$\boldsymbol{T}(l_2, l_1)$	5×5 transport matrix from l_1 to l_2
$T_{ij}(l_2, l_1) \ (i, j = 1, 2, \ldots, 5)$	elements of transport matrix
$\boldsymbol{A}_i = \boldsymbol{\sigma}^2[\boldsymbol{k}_i]\, \boldsymbol{T}^T(l_{i+1}, l_i)\, \boldsymbol{\sigma}^{-2}[\boldsymbol{e}_{i+1}]$	5×5 smoothing matrix at the i-th plane
θ_p	projected multiple scattering angle
$< \theta_p^2 >$	variance of the projected multiple scattering angle, eq. (43)

Table 3: Symbols used in the report.

References

[1] R.Frühwirth et al, *Data Analysis Techniques for High-Energy Physics*, 2nd edition, Cambridge University Press, Cambridge, 2000

[2] W. Wittek, EMC internal reports EMC/80/15, EMC/CSW/80/39, 81/13 and 81/18, Unpublished

[3] B.B. Niczyporuk, Track Fitting in a Inhomogeneous Magnetic Field, Report CEBAF-PR-91-004, (1991) Unpublished

[4] V. Innocente, M. Maire and E. Nagy, *GEANE: Average Tracking and Error Propagation Package*, CERN Program Library W5013-E (1991)

[5] V. Innocente and E. Nagy, *Trajectory fit in presence of dense materials*, Nucl. Instr. and Meth. A324(1993)297

[6] S. Gorbunov and I. Kisel, Nucl Inst. and Meth., A559(2006)148

[7] R.E. Kalman J. Basic Eng. 82(1961)34

[8] R. Frühwirth, Nucl. Instr. and Meth., A262(1987)444

[9] A. Rotondi and P. Montagna, Nucl. Instr. and Meth., B47(1990)215

[10] R. Frühwirth and M. Regler, Nucl. Instr. and Meth. A456(2001)369

[11] Particle Data Book, J. Phys. G 33(2006)1, see page 262

[12] Bruno Rossi, *High Energy Physics, Prentice Hall*, New York, 1952

[13] Glenn Cowan, *Statistical Data Analysis*, Clarendon Press, Oxford, 1998

[14] H. Bichsel, Nucl. Instr. and Meth. A562(2006)154

[15] GEANT3 manual, CERN proram library W5013 (1994)

[16] K. Lassilla-Perini and L. Urban, Nucl. Instr. and Meth., A362(1995)416